ANA CAROLINA SILVA GALDINO

MEMBERS OF THE *Fusarium solani* SPECIES COMPLEX (FSSC) ASSOCIATED WITH SUDDEN DEATH SYNDROME AND RED ROOT ROT OF SOYBEAN IN BRAZIL

LAVRAS–MG
2024

ANA CAROLINA SILVA GALDINO

MEMBERS OF THE *Fusarium solani* SPECIES COMPLEX (FSSC) ASSOCIATED WITH SUDDEN DEATH SYNDROME AND RED ROOT ROT OF SOYBEAN IN BRAZIL

Tese apresentada à Universidade Federal de Lavras, como parte das exigências do Programa de Pós-Graduação em Agronomia/Fitopatologia, área de concentração em Fitopatologia, para a obtenção do título de Doutora.

Prof. Dr. Ludwig H. Pfenning
Orientador

LAVRAS–MG
2024

Ficha catalográfica elaborada pelo Sistema de Geração de Ficha Catalográfica da Biblioteca Universitária da UFLA, com dados informados pelo(a) próprio(a) autor(a).

Galdino, Ana Carolina Silva.
Members of the *Fusarium solani* Species Complex (FSSC) associated with sudden death syndrome and red root rot of soybean in Brazil / Ana Carolina Silva Galdino. - 2024.
77 p. : il.

Orientador: Ludwig H. Pfenning.

Tese (Doutorado) - Universidade Federal de Lavras, 2024.
Bibliografia.

1. *Glycine max*. 2. molecular phylogeny. 3. species diversity. I. Pfenning, Ludwig H.. II. Título.

ANA CAROLINA SILVA GALDINO

MEMBERS OF THE *Fusarium solani* SPECIES COMPLEX (FSSC) ASSOCIATED WITH SUDDEN DEATH SYNDROME AND RED ROOT ROT OF SOYBEAN IN BRAZIL

MEMBROS DO COMPLEXO DE ESPÉCIES *Fusarium solani* (FSSC) ASSOCIADOS À SÍNDROME DA MORTE SÚBITA E PODRIDÃO VERMELHA DA RAIZ DA SOJA NO BRASIL

Tese apresentada à Universidade Federal de Lavras, como parte das exigências do Programa de Pós-Graduação em Agronomia/Fitopatologia, área de concentração em Fitopatologia, para a obtenção do título de Doutora.

APROVADA em 19 de Agosto de 2024.

Dr. Mário Lúcio V. de Resende	DFP, ESAL, UFLA
Dr. Adriano T. Bruzi	DAG, ESAL, UFLA
Dra. Katia V. Xavier	University of Florida, EUA
Dr. Guohong Cai	Purdue University, EUA

Prof. Dr. Ludwig H. Pfenning
Orientador

LAVRAS–MG
2024

Aos meus pais, José Antônio e Andréa, pelo amor, segurança e incentivo durante toda minha vida. Agradeço por sempre apoiarem minhas escolhas, por compartilharem da minha felicidade, pelos conselhos e por todas as oportunidades que puderam me dar. Sem vocês eu não chegaria até aqui. Obrigada!

DEDICO

AGRADECIMENTOS

À Universidade Federal de Lavras, ao Departamento de Fitopatologia e ao Programa de Pós-Graduação em Agronomia/Fitopatologia pela oportunidade de fazer parte da sua história.

À Coordenação de Aperfeiçoamento de Pessoal de Nível Superior (CAPES) e à Comissão CAPES-PrInt/UFLA pela concessão da bolsa de estudos no Brasil e no exterior.

Ao Prof. Dr. Ludwig H. Pfenning por me mostrar o que realmente é ser um Orientador. Obrigada por toda confiança, incentivo, orientação, amizade, ensinamentos e apoio durante meu tempo no Laboratório de Sistemática e Ecologia de Fungos (LSEF).

Ao técnico do LSEF, Edson Luis Rezende (*in memoriam*), pela ajuda, ensinamentos, convivência e amizade.

Aos demais professores do Programa de Pós-Graduação em Agronomia/Fitopatologia que contribuíram para o meu desenvolvimento acadêmico.

À Purdue University, aos meus orientadores Dr. Guohong Cai e Dr. Jin-Rong Xu, técnicos e colegas do Department of Botany and Plant Pathology pela oportunidade, orientação e ajuda durante uma experiência incrível no exterior.

Ao Prof. Dr. Mário Lúcio V. de Resende (DFP-UFLA), Prof. Dr. Adriano Bruzi (DAG-UFLA), Prof. Dra. Katia V. Xavier (University of Florida, EUA) e Prof. Dr. Guohong Cai (Purdue University, EUA) por comporem a banca avaliadora deste trabalho.

Aos meus pais, José Antônio e Andréa, e irmãos, Carlos Henrique e Maria Laura, por todo amor e incentivo.

Aos amigos que fiz durante essa jornada e aos que ajudaram no desenvolvimento deste trabalho.

RESUMO

O Brasil é o maior produtor mundial de soja. Duas importantes doenças dessa cultura são a síndrome da morte súbita (SDS) e podridão vermelha da raiz (PVR). Os agentes causais dessas doenças variam, porém, todos são membros do Complexo de Espécies *Fusarium solani* (FSSC), um grupo diverso de espécies filogenéticas que são patogênicas a várias espécies agrícolas. Os sintomas da SDS podem ser divididos em radiculares e foliares. Enquanto os sintomas nas raízes caracterizam-se por necrose e podridão dos tecidos, nas folhas observa-se o desenvolvimento de clorose e necrose internerval, oriundo da ação de fitotoxinas produzidas pelo patógeno nas raízes. O presente trabalho está dividido em 5 capítulos. No primeiro, é feita a apresentação e caracterização do problema. No segundo, é apresentado o manuscrito do artigo "Five *Fusarium solani* species are associated with sudden death syndrome of soybean in Brazil". Neste trabalho obtivemos 36 isolados de *Fusarium* de diferentes regiões produtoras de soja no Brasil e, através de análise filogenética, evidenciamos que dentre estes isolados temos representantes de 5 espécies de dois Clados do FSSC, sendo elas *F. paranaense*, *F. solani*, *F. brasiliense*, *F. crassistipitatum* e *F. tucumaniae*. Com a execução de teste de patogenicidade, confirmamos que os representantes das diferentes espécies de *Fusarium* apesar de pertencerem a diferentes Clados, todos são patogênicos e induzem sintomas foliares e radiculares semelhantes em plantas de soja. No terceiro capítulo, é apresentado um projeto executado durante o intercâmbio na Purdue University - EUA onde foi criado com sucesso três vetores para a edição genética de *F. virguliforme* através do silenciamento de dois genes (FvTox1 e FvNIS1) responsáveis pela codificação de duas fitotoxinas que induzem os sintomas foliares da SDS. As atividades descritas no quarto capítulo referentes à transformação genética de *F. virguliforme* via ATMT também foram executadas na Purdue University - EUA. Por fim, o quinto capítulo refere-se a um projeto iniciado no exterior e finalizado na UFLA onde foi identificado por PCR a presença de FvTox1 e FvNIS1 no genoma de outras espécies membro do FSSC que até então haviam sido identificados apenas em *F. virguliforme*.

Palavras-chave: *Glycine max*, filogenia molecular, diversidade de espécies, fitotoxinas.

ABSTRACT

Brazil is the world's largest producer of soybeans. Two important diseases of this crop are sudden death syndrome (SDS) and red root rot (RRR). The causal agents of these diseases vary, but they are all members of the *Fusarium solani* Species Complex (FSSC), a diverse group of phylogenetic species that are pathogenic to several agricultural crops. While root symptoms are characterized by necrosis and tissue rot, in the leaves the development of chlorosis and interveinal necrosis is observed, resulting from the action of phytotoxins produced by the pathogen in the roots. This work is divided into 5 chapters. The first presents and characterizes the problem. The second presents the manuscript of the article "Five *Fusarium solani* species are associated with sudden death syndrome of soybean in Brazil". In this work, we obtained 36 *Fusarium* isolates from different soybean-producing regions in Brazil and, through phylogenetic analysis, we showed that among these isolates we have representatives of 5 species from two FSSC Clades, namely *F. paranaense*, *F. solani*, *F. brasiliense*, *F. crassistipitatum* and *F. tucumaniae*. By performing a pathogenicity test, we confirmed that the representatives of the different *Fusarium* species, despite belonging to different FSSC Clades, are all pathogenic and induce similar foliar and root symptoms in soybean plants. In the third chapter, we present a project executed during the exchange at Purdue University - USA, where three vectors were successfully created for the genetic editing of *F. virguliforme* through the silencing of two genes (FvTox1 and FvNIS1) responsible for the encoding of two phytotoxins that induce the foliar symptoms of SDS. The activities described in the fourth chapter regarding the genetic transformation of *F. virguliforme* via ATMT were also carried out at Purdue University - USA. Finally, the fifth chapter refers to a project initiated abroad and completed at UFLA where the presence of FvTox1 and FvNIS1 in the genome of other FSSC member species was confirmed by PCR, which until then had only been identified in *F. virguliforme*.

Key-words: *Glycine max*, molecular phylogeny, species diversity, toxins.

INDICADORES DE IMPACTO

Estudamos a diversidade do gênero *Fusarium*, que ocorre em associação com plantas cultivadas e da vegetação natural. A identificação das espécies de acordo com conceitos modernos é um prerrequisito para o desenvolvimento de diversas tecnologias. Verificamos a distribuição em território nacional, identificamos seus hospedeiros e seu comportamento como patógeno, endófito ou produtor de micotoxinas. O fenômeno da patogenicidade é resultado da interação entre o fungo e a planta hospedeira, influenciado ainda por solo e clima. A prática de uma agricultura tropical altamente diversificada, tecnológica e inovadora no Brasil resulta em variações consideráveis e relevantes dessa interação. Os resultados gerados dão suporte à diagnose e ao monitoramento de doenças, à implementação de estratégias de controle, integrando uso de produtos químicos e biológicos, e ainda ao desenvolvimento de germoplasma vegetal com resistência genética. Representam prerrequisito indispensável para o desenvolvimento de tecnologia de detecção por PCR, baseada em polimorfismo único de DNA do organismo alvo.

IMPACT INDICATORS

We are investigating the diversity of the genus *Fusarium*, which occurs in association with cultivated plants and natural vegetation. Species identification according to modern concepts is a prerequisite for the development of various technologies. We verified its distribution throughout the country, identified its hosts and its behavior as a pathogen, endophyte or producer of mycotoxins. The phenomenon of pathogenicity is the result of the interaction between the fungus and the host plant, also influenced by soil and climate. The practice of highly diversified, technological and innovative tropical agriculture in Brazil results in considerable and relevant variations. The results generated support the diagnosis and monitoring of diseases, the implementation of control strategies, integrating the use of chemical and biological products, but also the development of plant germplasm with genetic resistance. They represent an indispensable prerequisite for the development of PCR detection technology, based on unique DNA polymorphisms of the target organism.

LISTA DE TABELAS

LISTA DE FIGURAS

SUMÁRIO

CHAPTER 1 – STATE OF THE ART

1. INTRODUCTION

Sudden death syndrome (SDS) and red root rot (RRR) are important diseases of soybean (*Glycine max* L. Merr.) due to their high potential for damage and difficulty of control. Both diseases have species of the *Fusarium solani* Species Complex (FSSC) as the causal agents and these pathogens are restricted to the root system, where they infect the plant. SDS symptoms are divided into foliar and root symptoms. Infected roots present necrosis and darkening of the tissues that can extend to the lower parts of the stem. The foliar symptom, characterized by chlorosis and interveinal necrosis, also known as "*folha carijó*" in Brazil, is usually visible from the end of the reproductive stage, most often after flowering, and can lead to early defoliation and plant death (Hartman et al. 2015). In contrast, RRR symptoms are restricted only to root rot and tissue discoloration that can also lead to plant death, i.e., infected plants do not exhibit any foliar symptoms (Costa et al. 2016).

Fusarium solani Species Complex (FSSC) is composed of more than 60 phylogenetic species distributed in 3 Clades. Clade 2 groups pathogenic species of legumes. Clade 3 has the largest number of pathogenic species to different agricultural crops, opportunistic pathogens of humans and animals, and decomposer species. Finally, Clade 1 has two species from New Zealand (O'Donnell 2000; Zhang et al. 2006; O'Donnell et al. 2008; Nalim et al. 2011; Schroers et al. 2016). The causal agents of SDS, *F. virguliforme*, *F. tucumaniae*, *F. brasiliense* and *F. crassistipitatum*, are grouped in Clade 2 (Aoki et al. 2003, 2005, 2012), while *F. paranaense*, the causal agent of RRR, belongs to Clade 3 of the FSSC (Costa et al. 2016).

SDS occurrence is confirmed in 6 countries in the world; USA, Canada, Argentina, Brazil, Malaysia and South Africa (Anderson; Tenuta 1998; Aoki et al. 2003, 2005, 2012; Scandiani et al. 2004, 2012; O'Donnell et al. 2010; Chehri et al. 2014; Tewoldemedhin et al. 2014, 2017; Cummings et al. 2018; Wang et al. 2019). *Fusarium virguliforme* has been reported as the causal agent of SDS in North America, being the main agent of this disease in the USA (Roy 1997; Rupe et al. 2001; Aoki et al. 2003), however, this species has apparently never been found in Brazil. In South America, *F. tucumaniae* and *F. brasiliense* are the main causal agents of SDS, respectively, in Argentina and Brazil (Aoki et al. 2005, 2012; O'Donnell et al. 2010). In Brazil, in addition to *F. brasiliense* and *F. tucumaniae*, *F. crassistipitatum* has also been reported as a causal agent of SDS (Aoki et al. 2012), while *F. paranaense* is reported as the causal agent of RRR (Costa et al. 2016).

2. BACKGROUND

2.1. *Fusarium solani* Species Complex

FSSC, a term coined by O'Donnell (2000), refers to a group of over 60 phylogenetic species. These species can be pathogenic to various agricultural crops, be opportunistic pathogens of humans and animals, and some are decomposers found in soil or plant debris (O'Donnell 2000; Zhang et al. 2006; O'Donnell et al. 2008; Nalim et al. 2011; Schroers et al. 2016; Geiser et al. 2021).

Members of this complex can be homothallic or heterothallic, but the sexual phase is known in only one-third of the species (O'Donnell, 2000; O'Donnell et al. 2008) and most species have been studied as plant pathogens (Coleman, 2016). Among the heterothallic species, seven have been classified as mating populations (MP I - VII) producing a sexual morph in nature or in lab crossings (Matuo; Synder, 1973) but each of them also represents a phylogenetic species (O'Donnell, 2000). The pathogenic species of this complex include some of the plant pathogens that are associated with root rots in more than 100 agricultural crops (Kolattukudy; Gamble, 1995).

Molecular phylogeny separates the species into three clades. Clade 1 is composed of *F. plagianthi* and *F. illudens*, species apparently endemic to New Zealand. Clade 2 groups at least 8 legume-pathogenic species that may be biogeographically linked to South America (O'Donnell 2000), including *F. virguliforme*, *F. tucumaniae*, *F. brasiliense* and *F. crassistipitatum*, the causal agents of SDS (Aoki et al. 2003). Finally, Clade 3 is the largest and most diverse group, with soil-borne species, plant pathogens and opportunistic pathogens of humans and animals (O'Donnell 2000; Zhang et al. 2006; O'Donnell et al. 2008; Nalim et al. 2011). This Clade is composed of at least 35 phylogenetic species and *F. paranaense*, the causal agent of RRR (Costa et al. 2016).

There is a consensus in the scientific community that FSSC is part of the genus *Fusarium* (O'Donnell et al. 2013, 2020; Geiser et al. 2021); however, the taxonomy of this group is still a topic of discussion. Following the concept of one fungus: one name (Norvell 2011), Geiser et al. (2013) proposed that the name *Fusarium* should be used for all members of this monophyletic group without the use of the telemorphic name for species that do have a sexual morph. Thus, there would be a standard in the nomenclature, especially since the species of this complex that do have a sexual morph have already been named as *Nectria*, *Neocosmospora* and *Haematonectria*. In contrast, recent publications referring to FSSC as species of the genus *Neocosmospora* contribute to the taxonomic debate between the two sides of the community, reinforcing the lack of a nomenclature standard, making communication among users, scientists

and regulatory agencies difficult (Lombard et al. 2015; Sandoval-Denis; Crous 2018; Sandoval-Denis et al. 2019; O'Donnell et al. 2020).

2.2. Soybean in Brazil

Soybean (*Glycine max* L. Merr.), member of the Fabaceae family and native to East Asia, is one of the world's main agricultural crops, as it is an important source of vegetable oil and protein for both human and animal consumption (Medic et al., 2014). This crop was introduced in 1882 in Bahia, Northeast region of Brazil, but the cultivars at that time were not adapted to the region's tropical climate. Therefore, until 1980, soybean production was concentrated in the South region of the country. From 1980 onwards, its cultivation expanded to the Central-West region thanks to the development of cultivars adapted to the region's conditions, and in the 2000s, to the North of the country (Cattelan; Dall'agnol, 2018). Currently, soybean leads the Brazilian agricultural scene in terms of planted area and production, with 46,020.2 thousand ha and 147,336.6 thousand tons in the 2023/24 season, respectively. Mato Grosso State is the largest producer in the country (39.34 million tons) and Bahia State has the highest productivity (3,780 kg/ha) (CONAB, 2024).

Several biotic factors can negatively impact soybean productivity and quality. It is estimated that more than 300 pathogen species can attack this crop worldwide, with a limited number capable of causing economic damage (Hartman et al., 1999). The occurrence of these diseases is influenced by the cultivar, environmental conditions, history of diseases in the area, previous crops, and management practices (Mueller et al., 2016). The level of economic damage due to diseases depends on the pathogen, affected tissue type, number of infected plants, disease severity, environmental conditions, level of susceptibility and/or resistance of the plant, and stage of development (Hartman; Hill, 2010). In Brazil, due to the tropical climate and cultivation over large areas, soybean producers face a great challenge in controlling soybean diseases (Cattelan; Dall'agnol, 2018).

2.3. Sudden death syndrome of soybean

Soybean sudden death syndrome is one of the main diseases affecting the productivity of this crop in North and South America (Rodriguez et al. 2021). The causal agents of SDS are known as *F. virguliforme*, *F. tucumaniae*, *F. brasiliense* and *F. crassistipitatum*, members of Clade 2 of the FSSC (Aoki et al. 2003, 2005, 2012). SDS occurrence is confirmed in Argentina (Aoki et al. 2003; Scandiani et al. 2012), USA (Aoki et al. 2003; O'Donnell et al. 2010; Cummings et al. 2018; Wang et al. 2019), Canada (Anderson; Tenuta 1998), Malaysia (Chehri et al. 2014) and South Africa (Tewoldemedhin et al. 2014, 2017).

In Brazil, the presence of *F. brasiliense*, *F. crassistipitatum* and *F. tucumaniae* was confirmed in the early 2000. At that time, Brazilian isolates supplied by J. T. Yorinori, a former researcher at Empresa Brasileira de Pesquisa Agropecuária (EMBRAPA), were used in the process of describing those species (Aoki et al. 2003, 2005, 2012) and since then no new reports were made. *F. virguliforme* is the only SDS causing species never to be found in Brazil. In contrast, this is the main SDS causal agent in the USA (Roy 1997; Rupe et al. 2001; Aoki *et al*. 2003) that was first observed in 1971 in the state of Arkansas and after 1990, it was reported in most of the USA soybean-producing states (Roy 1997; Roy et al., 1997).

The initial SDS symptoms occur in the roots during infection by the fungus at the beginning of plant development, leading to necrosis and death of the tissue. The main root and the lower region of the stem of infected plants begin to present vascular discoloration that can be observed longitudinally. After colonization of the root, the pathogen begins to produce toxins that are translocated to the leaves where they induce the development of chlorosis and leaf necrosis (Jin et al., 1996; Brar et al., 2011; Abeysekara; Bhattacharyya, 2014) that are more easily observed in the field after the middle of the reproductive stage and generally after flowering. The leaves begin to present chlorotic spots that become necrotic in the interveinal tissue, and may become slightly misshapen and wrinkled. As the disease progresses, the leaves become necrotic with only the veins remaining green and may detach from the petioles when severely affected. Under specific conditions, the fungus can sporulate on the roots, and sporodochia, which are generally blue in color, can be observed on the surface of the tissue. The pathogen is commonly isolated from root tissue and is rarely found in the stem or aerial tissue of the plant, which, when infected, are easily removed from the soil (Hartman et al., 2015).

Initial infection is favored by high soil moisture, and foliar symptoms of SDS are more frequently observed in years with above-average rainfall (Leandro et al., 2013). In the field, abrupt transition zones can be observed between areas with high and low incidence of SDS and may be related to changes in soil conditions such as water retention capacity, which is directly related to soil type, fertility level, and compaction level. In addition, symptomatic plants are usually observed in groups in the area, and in areas that have already presented problems with SDS, there is a greater chance of the disease occurring again, depending on the weather conditions during crop development (Hartman et al., 2015). Severe SDS infections lead to premature defoliation, flower, pod abortion, and reduction in grain size, which cause productivity losses (Roy et al., 1997; Hartman et al., 2015). However, the level of loss due to

SDS depends on factors such as plant-pathogen interaction, climatic and soil conditions (Sanogo et al., 2001; Srour et al., 2017).

The management of SDS is challenging because it requires an integrated system approach including cultural practices, host resistance and chemical control. Long-term crop rotation, delayed planting, and cultural practices that favor greater aeration and less soil compaction can be used to reduce disease severity (Hershman et al., 1990; Vick et al., 2006; Westphal; Xing, 2011; Perez-Brandan et al., 2013; Marburger et al., 2016; Srour et al., 2017). However, the main alternatives for SDS management are the use of genetic resistance and seed treatment with fungicides. SDS genetic resistance is complex because it involves two types of resistance: root resistance to fungal colonization and foliar resistance to toxins (Kumawat et al., 2016; Chang et al., 2018), and to date, there are no commercial cultivars that are fully resistant to SDS.

Currently, the main active ingredient studied for the chemical control of this disease is fluopyram, a systemic nematicide and fungicide of the benzamide chemical group, which acts by inhibiting the succinate dehydrogenase complex II (SDHI). In the USA, since 2014 the commercial product Ilevo® (BASF) formulated with fluopyram has been available, which is capable of reducing the initial establishment of SDS, being proven effective against *F. virguliforme*, *F. brasiliense* and *F. tucumaniae* (Sang *et al*. 2018; Kandel *et al*. 2019; Sjarpe *et al*. 2020). In 2019, Saltro® (Syngenta), containing pidiflumetofen, an SDHI, as an active ingrediente, was registered in the USA and it has already been reported as promising in reducing the severity of the disease (Adee 2020). A third active ingredient, cyclobutyfluram (TYMIRIUM® technology; Syngenta), whose chemical structure is similar to fluopyram, also an SDHI, has been shown to be effective in seed treatment to control SDS (Lenzi et al., 2020), however the commercial product is not yet available. In Brazil, we have three fluopyram-based products available for soybean crops, Ilevo® (BASF), Attila® (BAYER) and Verango® prime (BAYER), however none of them are registered for the control of the causal agents of SDS (MAPA, 2024).

In addition to cultural management strategies and the use of chemical control, there are reports of the use of biological control agents such as *Bacillus subtilis*, *Pseudomonas fluorescens*, *Chryseobacterium vietnamense* (Pin Viso et al., 2016) and *Trichoderma harzianum* (Pimentel et al., 2020) in the management of SDS. In Brazil, three commercial products are available for the biological control of *F. solani* f. sp. *glycines* (old name of *F. virguliforme*): Arvatico (Syngenta), Baktillis (Mezfer Brazil) and Trichodermax EC (Novozymes), whose biological control agents are, respectively, *B. velezensis*, *B. subtillis* and *T. asperellum* (MAPA, 2024).

2.4. Red root rot of soybean

The causal agent red root rot of soybean is *F. paranaense*, a member of Clade 3 of the FSSC. This species was described by Costa et al. (2016) and can be differentiated from other FSSC species pathogenic to soybean through the use of the phylogenetic and biological species concept. The symptoms induced in soybean by *F. paranaense* are restricted to root rot and necrosis. Despite being an important new pathogen of soybean, there is still no information available on the epidemiology, distribution, host range and management of *F. paranaense*.

REFERENCES

ABEYSEKARA, N. S.; BHATTACHARYYA, M. K. Analyses of the Xylem Sap Proteomes Identified Candidate *Fusarium virguliforme* Proteinacious Toxins. **PLoS ONE**, v. 9, n. 5, p. e93667, 20 maio 2014.

ADEE, E. A. Effect of Saltro Soybean Seed Treatment on Sudden Death Syndrome in Kansas in 2019. **Kansas Agricultural Experiment Station Research Reports**, v. 6, n. 5, 1 jan. 2020.

ANDERSON, T. R.; TENUTA, A. U. First Report of *Fusarium solani* f. sp. *glycines* Causing Sudden Death Syndrome of Soybean in Canada. **Plant Disease**, v. 82, n. 4, p. 448–448, abr. 1998.

AOKI, T. et al. Sudden-death syndrome of soybean is caused by two morphologically and phylogenetically distinct species within the *Fusarium solani* species complex— *F. virguliforme* in North America and *F. tucumaniae* in South America. **Mycologia**, v. 95, n. 4, p. 660–684, jul. 2003.

AOKI, T.; O'DONNELL, K.; SCANDIANI, M. M. Sudden death syndrome of soybean in South America is caused by four species of *Fusarium* : *Fusarium brasiliense* sp. nov., *F. cuneirostrum* sp. nov., *F. tucumaniae*, and *F. virguliforme*. **Mycoscience**, v. 46, n. 3, p. 162–183, 1 jun. 2005.

AOKI, T.; SCANDIANI, M. M.; O'DONNELL, K. Phenotypic, molecular phylogenetic, and pathogenetic characterization of *Fusarium crassistipitatum* sp. nov., a novel soybean sudden death syndrome pathogen from Argentina and Brazil. **Mycoscience**, v. 53, n. 3, p. 167–186, 1 maio 2012.

BRAR, H. K.; SWAMINATHAN, S.; BHATTACHARYYA, M. K. The *Fusarium virguliforme* Toxin FvTox1 Causes Foliar Sudden Death Syndrome-Like Symptoms in Soybean. **Molecular Plant-Microbe Interactions®**, v. 24, n. 10, p. 1179–1188, out. 2011.

CATTELAN, A. J.; DALL'AGNOL, A. The rapid soybean growth in Brazil. **OCL**, v. 25, n. 1, p. D102, jan. 2018.

CHANG, H.-X. et al. Integration of sudden death syndrome resistance loci in the soybean genome. **TAG. Theoretical and applied genetics. Theoretische und angewandte Genetik**, v. 131, n. 4, p. 757–773, abr. 2018.

CHEHRI, K.; SALLEH, B.; ZAKARIA, L. *Fusarium virguliforme*, a soybean sudden death syndrome fungus in Malaysian soil. **Australasian Plant Disease Notes**, v. 9, n. 1, p. 128, 20 mar. 2014.

COLEMAN, J. J. The *Fusarium solani* species complex: ubiquitous pathogens of agricultural importance. **Molecular Plant Pathology**, v. 17, n. 2, p. 146–158, fev. 2016.

CONAB. Companhia Nacional de Abastecimento. **Acompanhamento da safra brasileira de grãos**. v.11 n. 10 p. 1-121. Safra 2023/24. Brasília: Companhia Nacional de Abastecimento. 2024. Available at: https://www.conab.gov.br/info-agro/safras/graos/boletim-da-safra-de-graos.

COSTA, S. S. et al. *Fusarium paranaense* sp. nov., a member of the *Fusarium solani* species complex causes root rot on soybean in Brazil. **Fungal Biology**, v. 120, n. 1, p. 51–60, jan. 2016.

CUMMINGS, J. A.; MYERS, K. L.; BERGSTROM, G. C. First Report of Sudden Death Syndrome of Soybean Caused by *Fusarium virguliforme* in New York. **Plant Disease**, v. 102, n. 10, p. 2036–2036, out. 2018.

GEISER, D. M. et al. One Fungus, One Name: Defining the Genus *Fusarium* in a Scientifically Robust Way That Preserves Longstanding Use. **Phytopathology®**, v. 103, n. 5, p. 400–408, maio 2013.

GEISER, D. M. et al. Phylogenomic Analysis of a 55.1-kb 19-Gene Dataset Resolves a Monophyletic *Fusarium* that Includes the *Fusarium solani* Species Complex. **Phytopathology®**, v. 111, n. 7, p. 1064–1079, jul. 2021.

HARTMAN, G. L. et al. (EDS.). **Compendium of soybean diseases and pests**. Fourth edition. St. Paul, Minnesota, EUA: APS Press, The American Phytopathological Society, 1999.

HARTMAN, G. L.; CHANG, H.-X.; LEANDRO, L. F. Research advances and management of soybean sudden death syndrome. **Crop Protection**, Ecology and management of *Fusarium* diseases. v. 73, p. 60–66, 1 jul. 2015.

HARTMAN, G. L.; HILL, C. B. Diseases of soybean and their management. At: **The Soybean**. [s.l.] CABI Publishing, p. 276–299, 2010.

HERSHMAN D. E. et al. Influence of planting date and cultivar on soybean sudden death syndrome in Kentucky. **Plant Disease** v. 74, p. 761–766, out. 1990.

JIN, H. et al. Characterization and Purification of a Phytotoxin Produced by *Fusarium solani,* the Causal Agent of Soybean Sudden Death Syndrome. **Phytopathology**, v. 86, n. 3, p. 277, dez 1996.

KANDEL, Y. R. et al. Effect of Seed Treatment and Foliar Crop Protection Products on Sudden Death Syndrome and Yield of Soybean. **Plant Disease**, v. 103, n. 7, p. 1712–1720, jul. 2019.

KOLATTUKUDY, P. E.; GAMBLE, D. L. *Nectria haematococca*: pathogenesis and host specificity in plant diseases. In: **Pathogenesis and host specificity in plant pathogenic fungi and nematodes**. Eds. Kohmoto, K., Singh, U. S. & Singh, R. P., p. 83–102, 1995.

KUMAWAT, G. et al. QTLomics in Soybean: A Way Forward for Translational Genomics and Breeding. **Frontiers in Plant Science**, v. 7, 21 dez. 2016.

LEANDRO, L. F. S. et al. Climatic and Environmental Trends Observed During Epidemic and Non-epidemic Years of Soybean Sudden Death Syndrome in Iowa. **Plant Health Progress**, v. 14, n. 1, p. 18, jan. 2013.

LENZI L. et al. Evaluación de tratamiento de semillas con TymiriumTM para el control del síndrome de la muerte súbita de la soja. In: **Congreso Argentino de Semillas and INTA**, Argentina. Available at: https://repositorio.inta.gob.ar/xmlui/bitstream/handle/20.500.12123/10336/INTA_CRBsAsNorte_EEAPergamino_Lenzi_L_Evaluacion_de_tratamiento_de_semillas_con_tymirium_para_el_control_del_sindrome_de_muerte_subita_soja.pdf?sequence=1&isAllowed=y. 2020

LOMBARD, L. et al. Generic concepts in *Nectriaceae*. **Studies in Mycology**, v. 80, p. 189–245, mar. 2015.

MAPA. Ministério da Agricultura, Pecuária e Abastecimento. **Agrofit: Sistema de agrotóxicos fitossanitários**. Brasília, DF, MAPA, Available at: https://agrofit.agricultura.gov.br/agrofit_cons/principal_agrofit_cons. 2003

MARBURGER, D. A.; SMITH, D. L.; CONLEY, S. P. Revisiting Planting Date and Cultivar Effects on Soybean Sudden Death Syndrome Development and Yield Loss. **Plant Disease**, v. 100, n. 10, p. 2152–2157, out. 2016.

MATUO, T.; SYNDER, W. C. Use of Morphology and Mating Populations in the Identification of Formae Speciales in Fusarium solani. **Phytopathology**, v. 63, n. 5, p. 562, 1973.

MEDIC, J.; ATKINSON, C.; HURBURGH, C. R. Current Knowledge in Soybean Composition. **Journal of the American Oil Chemists' Society**, v. 91, n. 3, p. 363–384, 1 mar. 2014.

MUELLER D. S. et al. (EDS.) 2016. **A Farmer's Guide to Soybean Diseases**. First edition. St. Paul, Minnesota, EUA. APS Press, The American Phytopathological Society. 2016.

NALIM, F. A. et al. New species from the *Fusarium solani* species complex derived from perithecia and soil in the old World tropics. **Mycologia** 103:1302–1330. mai 2011.

NORVELL, L. L. Fungal nomenclature. 1. Melbourne approves a new Code. **Mycotaxon**, v. 116, n. 1, p. 481–490, 9 set. 2011.

O'DONNELL, K. Molecular phylogeny of the *Nectria haematococca-Fusarium solani* species complex. **Mycologia**, v. 92, n. 5, p. 919–938, set. 2000.

O'DONNELL, K. et al. No to *Neocosmospora* : Phylogenomic and Practical Reasons for Continued Inclusion of the Fusarium solani Species Complex in the Genus *Fusarium*. **mSphere**, v. 5, n. 5, p. e00810-20, 28 out. 2020.

O'DONNELL, K. et al. Phylogenetic analyses of RPB1 and RPB2 support a middle Cretaceous origin for a clade comprising all agriculturally and medically important fusaria. **Fungal genetics and biology**, v. 52, mar. 2013.

O'DONNELL, K. et al. Soybean Sudden Death Syndrome Species Diversity Within North and South America Revealed by Multilocus Genotyping. **Phytopathology®**, v. 100, n. 1, p. 58–71, jan. 2010.

O'DONNELL, K. et al. Molecular phylogenetic diversity, multilocus haplotype nomenclature, and in vitro antifungal resistance within the *Fusarium solani* species complex**. Journal of clinical microbiology**, v. 46, n. 8, ago. 2008.

PEREZ-BRANDAN, C. et al. The effect of crop sequences on soil microbial, chemical and physical indicators and its relationship with soybean sudden death syndrome (complex of *Fusarium* species). **Spanish Journal of Agricultural Research**, v. 12, n. 1, p. 252–264, 9 dez. 2013.

PIMENTEL, M. F. et al. *Trichoderma* Isolates Inhibit *Fusarium virguliforme* Growth, Reduce Root Rot, and Induce Defense-Related Genes on Soybean Seedlings. **Plant Disease**, v. 104, n. 7, p. 1949–1959, jul. 2020.

PIN VISO, N. D. et al. In vitro antagonistic activity of native bacteria isolated from soils of the Argentine Pampas against *Fusarium tucumaniae* and *Fusarium virguliforme*. **African Journal of Microbiology Research**, v. 10, n. 27, p. 1031–1035, 21 jul. 2016.

RODRIGUEZ, M. C. et al. Current recommendations and novel strategies for sustainable management of soybean sudden death syndrome. **Pest Management Science**, v. 77, n. 10, p. 4238–4248, out. 2021.

ROY, K. W. *Fusarium solani* on Soybean Roots: Nomenclature of the Causal Agent of Sudden Death Syndrome and Identity and Relevance of *F. solani* form B. **Plant disease**, v. 81, n. 3, mar. 1997.

ROY, K. W. et al. Sudden Death Syndrome of Soybean. **Plant Disease**, v. 81, n. 10, p. 1100–1111, out. 1997.

RUPE, J. C. et al. Differentiation of the sudden death syndrome pathogen of soybean, *Fusarium solani* f.sp. *glycines*, from other isolates of *F. solani* based on cultural morphology, pathogenicity, and mitochondrial DNA restriction fragment length polymorphisms. **Canadian Journal of Botany**, v. 79, n. 7, p. 829–835, 1 jul. 2001.

SANDOVAL-DENIS, M.; CROUS, P. W. Removing chaos from confusion: assigning names to common human and animal pathogens in *Neocosmospora*. **Persoonia: Molecular Phylogeny and Evolution of Fungi**, v. 41, p. 109–129, dez. 2018.

SANDOVAL-DENIS, M.; LOMBARD, L.; CROUS, P. W. Back to the roots: a reappraisal of Neocosmospora. **Persoonia: Molecular Phylogeny and Evolution of Fungi**, v. 43, p. 90–185, 2019.

SANG, H. et al. Fluopyram Sensitivity and Functional Characterization of SdhB in the *Fusarium solani* Species Complex Causing Soybean Sudden Death Syndrome. **Frontiers in Microbiology**, v. 9, p. 2335, 2018.

SANOGO, S.; YANG, X. B. Relation of sand content, pH, and potassium and phosphorus nutrition to the development of sudden death syndrome in soybean. **Canadian Journal of Plant Pathology**, v. 23, n. 2, p. 174–180, jun. 2001.

SCANDIANI, M. M. et al. Aislamiento, identificación y daños asociados al síndrome de la muerte súbita en el cultivo de soja en Argentina. **Tropical Plant Pathology**, v. 37, p. 358–362, out. 2012.

SCANDIANI, M. et al. Recent Outbreak of Soybean Sudden Death Syndrome Caused by *Fusarium virguliforme* and *F. tucumaniae* in Argentina. **Plant disease**, v. 88, n. 9, set. 2004.

SCHROERS, H.-J. et al. Epitypification of *Fusisporium* (*Fusarium*) *solani* and its assignment to a common phylogenetic species in the *Fusarium solani* species complex. **Mycologia**, v. 108, n. 4, p. 806–819, 2016.

SJARPE, D. A. et al. Multi-location evaluation of fluopyram seed treatment and cultivar on root infection by *Fusarium virguliforme* , foliar symptom development, and yield of soybean. **Canadian Journal of Plant Pathology**, v. 42, n. 2, p. 192–202, 2 abr. 2020.

SROUR, A. Y. et al. Unraveling Microbial and Edaphic Factors Affecting the Development of Sudden Death Syndrome in Soybean. **Phytobiomes Journal**, v. 1, n. 2, p. 91–101, jan. 2017.

TEWOLDEMEDHIN, Y. T. et al. First Report of Soybean Sudden Death Syndrome Caused by *Fusarium virguliforme* in South Africa. **Plant Disease**, v. 98, n. 4, p. 569, abr. 2014.

TEWOLDEMEDHIN, Y. T. et al. Soybean SDS in South Africa is Caused by *Fusarium brasiliense* and a Novel Undescribed *Fusarium* sp. **Plant Disease**, v. 101, n. 1, p. 150–157, jan. 2017.

VICK, C. M. et al. Response of soybean sudden death syndrome to tillage and cultivar. **Canadian Journal of Plant Pathology**, v. 28, n. 1, p. 77–83, mar. 2006.

WANG, J. et al. Soybean Sudden Death Syndrome Causal Agent *Fusarium brasiliense* Present in Michigan. **Plant Disease**, v. 103, n. 6, p. 1234–1243, jun. 2019.

WESTPHAL, A.; XING, L. Soil suppressiveness against the disease complex of the soybean cyst nematode and sudden death syndrome of soybean. **Phytopathology**, v. 101, n. 7, p. 878–886, jul. 2011.

ZHANG, N. et al. Members of the *Fusarium solani* species complex that cause infections in both humans and plants are common in the environment. **Journal of Clinical Microbiology**, v. 44, n. 6, p. 2186–2190, jun. 2006.

CHAPTER 2 – RESEARCH PAPER

Five *Fusarium solani* species are associated with sudden death syndrome of soybean in Brazil

Ana Carolina Silva Galdino[1] and Ludwig H. Pfenning[1*]

[1]Departamento de Fitopatologia, Universidade Federal de Lavras, 37200-900, Lavras, Minas Gerais, Brazil

*Corresponding author: Ludwig H. Pfenning, e-mail: ludwig@ufla.br

Manuscript prepared according to the standard of Plant disease

ABSTRACT

Sudden death syndrome and red root rot are important diseases of soybean and they have different members of the *Fusarium solani* species complex (FSSC) as causal agents. Our objectives in this work were to define the FSSC species that are associated with soybean in Brazil through molecular phylogeny, to confirm their pathogenicity and evaluate if their symptomatology differs between the FFSC Clades. We obtained 36 isolates from different soybean producing regions. With molecular phylogeny analysis based on the second largest subunit of RNA polymerase (RPB2) and intergenic region of anonymous loci 44 (L44) gene fragments, their species were defined as *F. paranaense* (n = 16), *F. solani* FSSC 5 (n = 11), *F. brasiliense* (n = 2), *F. crassistipitatum* (n = 3) and *F. tucumaniae* (n = 4). When inoculated to soybean plants, all representative isolated of the five species were pathogenic and induced the typical disease symptoms characterized as interveinal foliar chlorosis, necrosis and root rot 35 days after inoculation. No statistical difference in the disease symptoms was observed among *Fusarium* species from the different FSSC Clades. Our results confirm the diversity of SDS causal agents in Brazil which should raise the attention of the community to expand their research of SDS genetic resistance and disease control focusing on the interaction of soybean with the different *F. solani* species present in Brazil.

Key-words: *Glycine max*, *Fusarium solani* species complex, molecular phylogeny, root rot.

1. INTRODUCTION

Fusarium solani species complex (FSSC) refers to the group of more than 60 phylogenetic species distributed in three Clades according to molecular phylogeny. Species from this complex can be opportunistic pathogens of human and animals, some species are decomposers being found in soil or plant materials debris and there are also pathogenic species to various agricultural crops (O'Donnell 2000; Zhang et al. 2006; O'Donnell et al. 2008; Nalim et al. 2011; Schroers et al. 2016).

Sudden death syndrome (SDS) and red root rot (RRR) are important soybean (*Glycine max* L. Merr.) diseases due to their high potential of damage. SDS can cause 100% yield losses (Roy et al. 1997; Hartman et al. 2015; Kandel et al. 2015) and its control is difficult (Kandel et al. 2015; Spampinato et al. 2021). Brazil is the world's greatest soybean producer with 147 million tons in 2023/24 (CONAB, 2024) however, knowledge about those diseases occurrence in Brazil is still limited. Both of them have species from FSSC as the causal agent and those pathogens are restricted to the root system, where they infect the plant.

SDS symptoms can be divided into foliar and root symptoms. Infected roots present tissue necrosis and browning discoloration that can extend to the lower part of stems. The foliar symptoms generally begin in the late reproductive cycle, most times after flowering, as interveinal chlorosis that expands and becomes necrotic, that in Brazil is known as "*folha carijó"*, leading to premature defoliation and plant death (Hartman et al. 2015). In contrast, the RRR symptoms are restricted to root rot and vascular discoloration that can also lead to plant death and, according to Costa et al. (2016), infected plants do not exhibit any foliar symptoms.

There are reports of the occurrence of SDS in the USA (Aoki et al. 2003; O'Donnell et al. 2010; Cummings et al. 2018; Wang et al. 2019), Canada (Anderson and Tenuta 1998), Argentina (Aoki et al. 2003; Scandiani et al. 2004, 2012), Malaysia (Chehri et al. 2014b) and South Africa (Tewoldemedhin et al. 2014, 2017). In North America, *F. virguliforme* is reported as the causal agent of SDS, being the main causal agent of this disease in the USA (Roy 1997; Rupe et al. 2001; Aoki et al. 2003), but this species has apparently never been found in Brazil. In South America, *F. tucumaniae* e *F. brasiliense* are reported as the main causal agents of SDS, respectively, in Argentina and Brazil (Aoki et al. 2005, 2012; O'Donnell et al. 2010). In Brazil, in addition to *F. brasiliense* and *F. tucumaniae*, *F. crassistipitatum* has also been reported as causal agent of SDS (Aoki et al. 2012), while *F. paranaense* has been reported as the RRR causal agent (Costa et al. 2016).

The foliar symptoms of SDS result from the action of toxins produced by the pathogen on the plant roots that are transported by the vascular system to the leaves (Hartman et al. 2015).

So far, only toxins produced by *F. virguliforme* have been characterized, such as a 17 kDa protein (Jin et al. 1996), the FvTox1 protein and virulence factor (Brar et al. 2011) and the FvNIS1 effector (Chang et al. 2016), which are directly related to the development of leaf chlorosis and necrosis in soybean. There are also other candidate toxins identified in *F. virguliforme* and *F. tucumaniae* culture filtrates (Xiang et al. 2015; Chang et al. 2016; Abeysekara et al. 2016) but not yet characterized. No reports are available regarding the production of toxins by the other causal agents of SDS and RRR in the literature.

Our objectives in this study were (i) to determine the *Fusarium solani* species that are associated with SDS and RRR of soybean in Brazil using molecular phylogeny analysis; (ii) to verify their pathogenicity to soybean; and (iii) to confirm if there are difference in symptoms induced by FSSC Clade 2 and Clade 3 species in association with soybean.

2. MATERIALS AND METHODS

2.1. Fungal isolates

The fungal strains were obtained from soybean samples with symptoms of SDS/RRR, i.e. leaves with interveinal chlorosis and necrosis and/or reddish spots on the root, from several Brazilian states where soybean is cultivated (Table 1). After removing soil excess, the roots were individually wrapped in paper towels, moistened with distilled water, placed in plastic bags, identified and stored at 10ºC for 4 days followed by 1 day at room temperature. After incubation, the roots were observed under stereo microscope to identify the presence of characteristic sporulation of FSSC. Direct isolation was performed by transferring these structures to Petri dishes (ø 60 mm) containing 2% malt extract agar (2% MA; 20 g of malt extract L^{-1}; Kasvi, Spain) media, which were then incubated at 25 ± 2ºC with 12 h of photoperiod.

For indirect isolation, 1 cm fragments of the transition region between sympthomatic and healthy root tissue were superficially disinfected by immersion in 70% ethanol for 1 min, followed by immersion in 1% NaOH for 2 min and rinsed in sterile distilled water. The fragments were dried on sterile filter paper, transferred to Petri dishes containing 2% MA and incubated at 25 ± 2ºC with 12 h of photoperiod. After, the samples were also observed under magnifying glass to identify the presence of characteristic sporulation of FSSC and transferred to Petri dishes with 2% MA. The isolates were deposited in the Coleção Micológica de Lavras (CML), Departamento de Fitopatologia, Universidade Federal de Lavras (UFLA), Lavras, Minas Gerais, Brazil (http://www.dfp.ufla.br/cml).

2.2. DNA extraction, PCR and sequencing

Isolates were grown in 2% malt extract broth for 3 days at room temperature under constant agitation in a rotary shaker (100 rpm). The DNA was extracted from fungal biomass using the Wizard® Genomic DNA purification kit (Promega, USA) following the manufacture's protocol and DNA quantification of samples was performed using NanoDrop One™ (ThermoFisher Scientific, USA).

PCR were performed using GoTaq® Colorless Master Mix (Promega, USA) following the manufacture's protocol. We amplified fragments from the second largest subunit of RNA polymerase (RPB2) using the primers 5F2 (GGG GWG AYC AGA AGA AGG C) and 7cR (CCC ATR GCT TGT YYR CCC AT) (Liu et al., 1999; Sung et al., 2007) for all isolates. Later, we amplified fragments from the intergenic region of anonymous loci 44 (L44) using the primers 44-1 (GTG AGG GCG TCG TGA AGA AT) and 44-2i (GGA ACG ATA GTT CAG ATG CTC) (Covert et al., 2007) only for the FSSC Clade 2 isolates. The PCR products were subjected to electrophoresis in 1% agarose gel stained with GelRed® (Biotium, USA) and visualized in a MiniBIS transilluminator (DNR Bio-Imaging Systems, Israel). The amplified fragments were purified and Paired-end sequenced in both directions by Psomagen (Rockville, USA).

2.3. Molecular phylogeny

Sequences were assembled using SeqAssem v. 07/2008 (Hepperle, 2004) and alignments were obtained using the ClustalW tool (Thompson et al., 1994) implemented in the MEGA 11 software (Kumar et al., 2018). Partial sequences of RPB2 and L44 from representative strains were compared with sequences from strains of other FSSC species (Table S1). Phylogenetic analysis was performed using Maximum Parsimony (MP) method for each gene and for the concatenated data set in MEGA 11 with 1000 bootstrap replications. Sequences from *F. illudens* (NRRL 22090) and *F. plagianthi* (NRRL 22632) were used as outgroup, according to O'Donnell et al. (2008), in the RPB2 tree. Alignment sequences consisted of 124 parsimony-informative sites out of 880 bp for RPB2; 28/2236 for L44 and 152/4161 for RPB2 + L44. The DNA sequences generated in this study were deposited in GenBank, NCBI (Table 1).

2.4. Pathogenicity test

For the pathogenicity test one isolate of each species from distinct geographic origin was selected (Table 1). Soybean plants from the cultivar M6410 IPRO were grown in 2 L plastic containers with a sterile mix of soil, sand and commercial substrate (Carolina Soil, Brazil) in a 1:1:1 ratio.

Inoculum preparation was performed according to Hartman et al. (1997). Sorghum grains (480 g per treatment) were immersed in distilled water for 12 h and autoclaved in two consecutive days for 1 h at 121ºC. Then, six mycelium plugs (ø 5 mm) of each isolate were transferred to the sorghum bags that were incubated for 15 days at 25 ± 2ºC with 12 h of photoperiod and daily mixed. Plant inoculation was performed using the inoculum layer methodology (Hartman et al., 1997). For this, the plastic containers were prepared with a layer of the soil mix, followed by a layer of 80 g of infested sorghum per repetition and a layer of the soil mix. The seeds were deposited equidistantly and covered with the last layer of soil mix. The control treatment was set up using the same steps described above but the sorghum grains were not infested. The experiment was conducted in a greenhouse at 25 ± 5ºC. The plants were irrigated as needed and fertilized every week with 15g of NPK 4-14-8.

The foliar disease symptoms evaluation was performed 35 days after inoculation (DAI) using the Huang and Hartman (1998) scale, varying from 1 to 5, where: 1 = no symptoms; 2 = light symptom development with mottling and mosaic (1 to 20% of foliage affected); 3 = moderate symptom development with interveinal chlorosis and necrosis (21 to 50% of foliage affected); 4 = heavy symptom development with interveinal chlorosis and necrosis (51 to 80% of foliage affected) and 5 = severe symptom development with interveinal chlorosis and necrosis and/or dead plants (81 to 100% of foliage affected). Root symptoms were also evaluated at 35 DAI by measuring internal root necrosis with a ruler.

The experiments were conducted in a completely randomized design with six replications per treatment and the experimental unit consisted in one plant. They were repeated twice independently and the values represented in this study are the average of them. The data were subjected to Shapiro-Wilk's normality test and Bartlett's homogeneity test ($p \leq 0.05$) followed by one-way ANOVA and Scott-Knott tests ($p \leq 0.05$) or Kruskal-Wallis and Dunn tests ($p \leq 0.05$) to compare, respectively, root necrosis and disease severity among treatments. Statistical analyses were performed using R v. 4.3.1 (R Core Team, 2023).

2.5. Evaluation of morphological markers

The evaluation of morphological markers was performed according to Aoki et al. 2003 and compared with the literature (Aoki et al. 2005, 2012; Costa et al., 2016; Schroers et al. 2016; Sandoval et al., 2019). The isolates were grown in Petri dish with potato dextrose agar (PDA) media incubated for 4 days in the dark at 25 ± 2ºC to evaluate the colony growth rate and for 10 days with 12h of photoperiod also at 25 ± 2ºC for evaluation of morphology and pigmentation of colonies. The size, number of septa and characteristics of the conidia, as well

as the observation of the characteristics of the conidiophores and production of chlamydospores was carried out after incubation of the isolates in a Petri dish with synthetic low nutrient agar (SNA) + carnation leaf media at 25 ± 2ºC with 12 h of photoperiod per 10-14 days. Measurements were made for 25-30 structures of each isolate.

3. RESULTS

3.1. Phylogenetic analysis

The phylogenetic analysis of 36 isolates based on the RPB2 gene revealed n = 27 members of Clade 3 and n = 9 members of Clade 2 of FSSC (Figure 1). In FSSC Clade 3, 16 isolates are grouped with reference sequences of *F. paranaense* while 11 isolates are grouped with reference sequences of *F. solani* FSSC 5. The remaining 9 isolates are members of FSSC Clade 2 however, only the RPB2 gene did not provide enough resolution to define species inside this Clade. The combined RPB2 + L44 genes phylogenetic analysis of the Clade 2 isolates revealed members of 3 species: *F. brasiliense* (n = 2), *F. crassistipitatum* (n = 3) and *F. tucumaniae* (n = 4) (Figure 2).

3.2. Pathogenicity test

All *F. solani* species used in the test were pathogenic to soybean plants but no significant differences in disease severity and root necrosis were observed between them (Table 2). The soybean plants inoculated with the different *F. solani* species reached on average the score of 2.9 out of 5 in the Huang and Hartman (1998) scale and root necrosis observed reached on average 1.4 cm at 35 DAI.

Foliar symptoms were first observed at 21 DAI as light mottling starting at the edge of the leaves, progressing to interveinal chlorosis and necrosis observed at the final evaluation at 35 DAI. In the roots we observed dark brown lesions or decay of the entire tap roots (Figure 3). Koch's postulates were completed through the re-isolation of the pathogens and confirming the sequence identity (RPB2 and L44). Plants used as the control group were asymptomatic.

3.3. Morphology of isolates

The isolates evaluated showed typical morphological characteristics of *F. solani*, such as long and slender monophialides, conidia production in false heads, smooth and rough chlamydospores, variable color of the colony in shades of white, beige, light brown or bluish, and sporodochia in cream, brown or blue color (Figure 4).

Fusarium paranaense colonies' growth rate on PDA were 6.5 to 8.6 mm a day and their color ranged from white to light brown, with beige, light brown and blue sporodochia. Macroconidia produced in sporodochia had a cylindrical to fusiform shape, with a slightly

protruding basal cell, 3 to 5 septa and size between 37 to 48 × 4 to 7.5 µm. Conidia produced in aerial mycelium presented oval, cylindrical to fusiform shape, with 0 to 4 septa and size between 12 to 37 × 5 to 7.5 µm. Chlamydospores with globose to subglobose shape, smooth and rough surface, solitary, terminal or intercalated with size between 7 to 8 × 6 to 8 µm were abundantly observed in some isolates

A beige to light brown coloration was observed in *F. solani* FSSC 5 colonies grown on PDA with sporodochia also in these colors. Colonies growth rate on PDA were 6.2 to 8.3 mm a day. Macroconidia produced in sporodochia presented falcate shape with slightly curved basal and apical cells, with 3 to 5 septa and 38 to 47 × 4 to 7.5 µm. Conidia produced in aerial mycelium also presented falcate to slightly curved shape, with 0 to 4 septa and 14 to 37 × 4 to 7.5 µm. Chlamydospores measuring 7 to 9 µm with globose shape and smooth surface were observed.

It was not possible to distinguish the FSSC Clade 2 strains at species level based only on the morphological characteristics. Colonies on PDA showed mycelial growth rate of 1.6 to 2.7 mm a day and their color ranged from white, beige and pale yellow with cream and blue sporodochia. Macroconidia produced in sporodochia presented a cylindrical to falcate shape, slightly curved, with a distinct basal cell, 3 to 5 septa and 55 to 67 × 6 to 7.5 µm. Macroconidia produced in aerial mycelium had the same shape and number of septa as the sporodochia conidia, however they had a slightly smaller size, 41 to 63 × 6 to 7.5 µm. Microconidia and chlamydospores were absent in the evaluated isolates.

4. DISCUSSION

In this study, five distinct phylogenetic species from FSSC Clades 3 and 2 were isolated from soybean plants collected in different geographic regions of Brazil. The majority (n = 22) of isolates were obtained from the Central-West (Mato Grosso, Mato Grosso do Sul and Goiás states) while the remaining samples came from the Southeast (n = 9; Minas Gerais state) and South (n = 5; Rio Grande do Sul state) region of the country. Our results confirm the association of two FSSC Clade 3 species, *F. paranaense* and *F. solani* FSSC 5, and three FSSC Clade 2 species, *F. brasiliense, F. crassistipitatum* and *F. tucumaniae*, with soybean plants. *F. virguliforme*, also a FSSC Clade 2 species, has still not being found in association with soybean in Brazil and in our view, expanding the sampling area in future studies is highly recommended to either confirm the presence or monitor the pathogen introduction especially because this species has been reported present in Argentina (Scandiani et al. 2004; O'Donnel et al. 2010).

According to Sandoval-Denis and Crous (2018) and Sandoval et al. (2019) the complete FSSC should be removed from the *Fusarium* genus into the *Neocosmospora* genus and the

earlier mentioned species should be named *N. falciformis* (*F. paranaense*), *N. solani* (*F. solani* FSSC 5) and *N. phaseoli* (*F. brasiliense*, *F. crassistipitatum*, *F. tucumaniae* and *F. virguliforme*). Nevertheless, this change has been severely refuted by the *Fusarium* scientific community through the allegation of incorrect interpretation of Geiser et al. (2013) and its support by the longstanding use of FSSC name among plant pathologists, medical mycologists, quarantine officials, regulatory agencies, students and researchers with a stake in its taxonomy (O'Donnell et al. 2020; Geiser et al. 2021). Here, we opted to continue the use of the name of the genus *Fusarium* which is supported by a robust taxonomy that facilitates communication.

Fusarium paranaense, a FSSC Clade 3 species described by Costa et al. (2016) as causal agent of red root rot of soybean is considered to be a sibling species of *F. falciforme* (FSSC 3 + 4). However, *F. paranaense* can be distinguished from other soybean pathogens inside FSSC by both phylogenetic and biological species concept (Costa et al. 2016). With that in mind, we chose to keep this name when referring to the isolates that in our phylogenetic analysis grouped with *F. paranaense* reference species (CML 860 and CML 1830). The isolates obtained in the present work exhibited variability in colony color and their morphological characteristics are consistent with the literature (Costa et al. 2016). Due to different sampling geographic origins, in our work *F. paranaense* was mostly found in the Mato Grosso state (Central-West region) which currently is responsible for the highest soybean productivity of Brazil (39,3 million tons in 2023/24) (CONAB, 2024) while Costa et al. (2016) reported that this species was more frequently in the Paraná state (South region). Despite the high genetic variability due to sexual reproduction of *F. paranaense* and its presence in all major soybean producing regions of the country, information regarding plant-pathogen interaction, disease epidemiology, management, host range and even economic potential damage are not available.

Fusarium solani FSSC 5 is also a member of the FSSC Clade 3, considered to be the largest and most diverse FSSC Clade because it includes species that are associated with soil and plants, plus the ones able to cause opportunistic infections in humans and animals and those that have saprophytic behavior (O'Donnell 2000; Zhang et al. 2006; O'Donnell et al. 2008). Members of the *F. solani* FSSC 5 species have been mostly reported as clinical opportunistic pathogens associated with infectious diseases of humans and animals (O'Donnell et al. 2008) yet, there are reports of *F. solani* FSSC 5 association with important agricultural crops such as potato (Chehri et al. 2014a; Schroers et al. 2016), strawberry (De La Lastra et al. 2019), cucurbits (Sabahi et al. 2023) and legumes (Chitrampalam and Nelson 2016; Wang et al. 2019; Dell'Olmo et al. 2023). To the best of our knowledge, here is reported for the first time the association of *F. solani* FSSC 5 with soybean plants in Brazil. The ecology of these clinically

important isolates in agriculturally important soils, especially in the rhizosphere of soybean and other major crops, remains to be determined and Chitrampalam and Nelson (2016) suggests that isolates belonging to *F. solani* FSSC 5 species could be facultative plant pathogens.

The Clade 2 species, *F. brasiliense*, *F. crassistipitatum* and *F. tucumaniae*, were the least frequent ones to be found in association with soybean plants in this work. The common morphological character of those species is the formation of plural types of conidia, especially on aerial conidiophores (Aoki et al. 2003, 2005, 2012). *F. brasiliense* is characterized by septate cylindrical sporodochial conidia with rounded ends usually shorter than the ones produced by *F. tucumaniae* (Aoki et al. 2005). *F. crassistipitatum* typically produces sporodochial conidia with a rostrate apical cell and a slightly protruding basal foot cell, however, its dimensions overlap with *F. brasiliense*, and accorging to Aoki et al. (2012) it lacks diagnostic value. *F. tucumaniae* produces long, slender, cylindrical and gently curved or sometimes falcate, with an acute apical cell and a distinct basal sporodochial conidia that differentiate it from other FSSC Clade 2 species that causes SDS (Aoki et al. 2003, 2005). Regardless of the sporodoquial conidia morphology description in literature, we were not able to differentiate our FSSC Clade 2 isolates by it and it is known that the examination and interpretation of morphological characters can vary from person to person, elevating the subjectiveness and difficulty of the morphology-alone based identification of species (Jeewon et al. 2002; Promputtha et al. 2005, 2007; Senanayake et al. 2020). The different FSSC Clade 2 species colony color on PDA were often similar and not useful for species recognition as reported by Aoki et al. (2005), however, we could clearly see a difference in growth rate between FSSC Clade 3 and Clade 2 isolates (on average 7.4 vs 2.1 mm a day respectively), which may be established as a parameter to separate those species in the FSSC Clades.

Our pathogenicity test confirmed that the five *F. solani* species were able to induce the peculiar SDS foliar symptoms of chlorotic mottling, interveinal chlorosis and necrosis and also root rot of soybean plants with no statistical difference among species. We know that more than one phytotoxin is associated with the development of SDS foliar symptoms (Baker and Nemec 1994; Jin et al. 1996; Brar et al. 2011; Pudake et al. 2013; Chang et al. 2016). In spite of the variability of SDS causal agent, the majority of studies about plant-pathogen interaction in this pathosystem is focused only in *F. virguliforme*, therefore, one can only suppose the same is valid to the other SDS agents due to their species similarity. Thus, it is paramount that future SDS phytotoxins studies focus on the other *F. solani* species that are causal agents of this disease.

It could be argued that the foliar symptoms exhibited by the soybean plants inoculated with distinct *F. solani* species in our trial visually differ in intensity and do not visually correlate with the severity of root necrosis. But we should consider the possibility that species within the FSSC can display varying degrees of aggressiveness (Chitrampalam and Nelson 2016), some fungal isolates could be effective in colonizing the host root and may not be good toxin producers and vice versa (Tewoldemedhin et al. 2017) and finally, the appearance and severity of typical SDS foliar disease symptoms cannot always be associated with the fungal quantity in roots (Wang et al. 2019). Opposed to Costa et al. (2016), soybean plants inoculated with *F. paranaense* did exhibit foliar symptoms, *i.e.* interveinal chlorosis and necrosis, in our trials and since we have up to none information about *F. paranaense* interaction with soybean, research on this topic is an excellent challenge for the future.

The present study demonstrated that there are five pathogenic *F. solani* species associated with soybean plants in Brazil. The knowledge of the economically important causal agents of SDS and recognition of its genetic diversity are essential to the establishment of molecular surveillance programs to monitor pathogen dissemination due to world trade and foment disease control research (O'Donnel 2000, Aoki et al. 2005). SDS genetic resistance is complex because there are two components, the root resistance to fungal colonization and foliar resistance to fungal toxins (Kumawat et al. 2016; Chang et al. 2018) however, host resistance and cultivar selection are still the main strategies to manage the disease (Hartman et al. 2015). Most of the research in the world has been done with the FSSC Clade 2 species, *F. virguliforme*, that does not occur in Brazil as opposed to *F. brasiliense*, *F. crassistipitatum* and *F. tucumaniae*, and the FSSC Clade 3 species, *F. paranaense*, that can also cause SDS. Future studies should diversify and investigate the role that the other *F. solani* species, *i.e*. *F. paranaense*, *F. brasiliense*, *F. crassistipitatum* and *F. tucumaniae*, plays in the sudden death of soybean.

5. ACKNOWLEDGMENTS

ACSG is thankful for the PhD degree scholarship provided by Coordination for the Improvement of Higher Education Personnel (CAPES). We thank Edson L. Rezende, Gabriel S. Miguel and João Victor R. Corso for their assistance during the execution of this work.

6. REFERENCES

Abeysekara, N. S., Swaminathan, S., Desai, N., Guo, L., and Bhattacharyya, M. K. 2016. The plant immunity inducer pipecolic acid accumulates in the xylem sap and leaves of soybean seedlings following *Fusarium virguliforme* infection. Plant Science. 243:105–114

Anderson, T. R., Tenuta, A. U. 1998. First Report of *Fusarium solani* f. sp. *glycines* Causing Sudden Death Syndrome of Soybean in Canada. Plant Disease. 82:448–448

Aoki, T., O'Donnell, K., Homma, Y., and Lattanzi, A. R. 2003. Sudden-death syndrome of soybean is caused by two morphologically and phylogenetically distinct species within the *Fusarium solani* species complex - *F. virguliforme* in North America and *F. tucumaniae* in South America. Mycologia. 95:660–684

Aoki, T., O'Donnell, K., and Scandiani, M. M. 2005. Sudden death syndrome of soybean in South America is caused by four species of *Fusarium*: *Fusarium brasiliense* sp. nov., *F. cuneirostrum* sp. nov., *F. tucumaniae*, and *F. virguliforme*. Mycoscience. 46:162–183

Aoki, T., Scandiani, M. M., and O'Donnell, K. 2012. Phenotypic, molecular phylogenetic, and pathogenetic characterization of *Fusarium crassistipitatum* sp. nov., a novel soybean sudden death syndrome pathogen from Argentina and Brazil. Mycoscience. 53:167–186

Baker, R. A. and Nemec, S. 1994. Soybean sudden death syndrome: Isolation and identification of a ney phytotoxin from cultures of the causal agent, *Fusarium solani*. Phytopathology 84:1144

Brar, H. K., Swaminathan, S., and Bhattacharyya, M. K. 2011. The *Fusarium virguliforme* Toxin FvTox1 Causes Foliar Sudden Death Syndrome-Like Symptoms in Soybean. MPMI. 24:1179–1188

Chang, H.-X., Domier, L. L., Radwan, O., Yendrek, C. R., Hudson, M. E., and Hartman, G. L. 2016. Identification of Multiple Phytotoxins Produced by *Fusarium virguliforme* Including a Phytotoxic Effector (FvNIS1) Associated With Sudden Death Syndrome Foliar Symptoms. MPMI. 29:96–108

Chang, H.-X., Roth, M. G., Wang, D., Cianzio, S. R., Lightfoot, D. A., Hartman, G. L., et al. 2018. Integration of sudden death syndrome resistance loci in the soybean genome. Theor Appl Genet. 131:757–773

Chehri, K., Ghasempour, H. R., and Karimi, N. 2014a. Molecular phylogenetic and pathogenetic characterization of *Fusarium solani* species complex (FSSC), the cause of dry rot on potato in Iran. Microbial Pathogenesis. 67–68:14–19.

Chehri, K., Salleh, B., and Zakaria, L. 2014b. *Fusarium virguliforme*, a soybean sudden death syndrome fungus in Malaysian soil. Australasian Plant Dis. Notes. 9:128

Chitrampalam, P., and Nelson, B. 2016. Multilocus phylogeny reveals an association of agriculturally important *Fusarium solani* species complex (FSSC) 11, and clinically important FSSC 5 and FSSC 3 + 4 with soybean roots in the north central United States. Antonie van Leeuwenhoek. 109:335–347

CONAB – Companhia Nacional de Abastecimento 2024. Acompanhamento da safra brasileira de gãos. v.11 n. 10 p. 1-121. Safra 2023/24. Brasília: Companhia Nacional de Abastecimento. 2024. Available at: https://www.conab.gov.br/info-agro/safras/graos/boletim-da-safra-de-graos. Accessed on: 21 jun. 2024.

Costa, S. S., Matos, K. S., Tessmann, D. J., Seixas, C. D. S., and Pfenning, L. H. 2016. *Fusarium paranaense* sp. nov., a member of the *Fusarium solani* species complex causes root rot on soybean in Brazil. Fungal Biology. 120:51–60

Covert, S. F., Aoki, T., O'Donnell, K., Starkey, D., Holliday, A., Geiser, D. M., et al. 2007. Sexual reproduction in the soybean sudden death syndrome pathogen *Fusarium tucumaniae*. Fungal Genetics and Biology. 44:799–807

Cummings, J. A., Myers, K. L., and Bergstrom, G. C. 2018. First Report of Sudden Death Syndrome of Soybean Caused by *Fusarium virguliforme* in New York. Plant Disease. 102:2036–2036

De La Lastra, E., Villarino, M., Astacio, J. D., Larena, I., De Cal, A., and Capote, N. 2019. Genetic Diversity and Vegetative Compatibility of *Fusarium solani* Species Complex of Strawberry in Spain. Phytopathology®. 109:2142–2151

Dell'Olmo, E., Zaccardelli, M., and Sigillo, L. 2023. Occurrence of strains belonging to *Fusarium solani* species complex causing yellows on chickpea (*Cicer arietinum* (L.)) in Italy. J Plant Pathol. 105:623–623

Geiser, D. M., Al-Hatmi, A. M. S., Aoki, T., Arie, T., Balmas, V., Barnes, I., et al. 2021. Phylogenomic Analysis of a 55.1-kb 19-Gene Dataset Resolves a Monophyletic *Fusarium* that Includes the *Fusarium solani* Species Complex. Phytopathology®. 111:1064–1079

Geiser, D. M., Aoki, T., Bacon, C. W., Baker, S. E., Bhattacharyya, M. K., Brandt, M. E., et al. 2013. One Fungus, One Name: Defining the Genus *Fusarium* in a Scientifically Robust Way That Preserves Longstanding Use. Phytopathology®. 103:400–408

Hartman, G. L., Chang, H.-X., and Leandro, L. F. 2015. Research advances and management of soybean sudden death syndrome. Crop Protection. 73:60–66

Hartman, G. L., Huang, Y. H., Nelson, R. L., and Noel, G. R. 1997. Germplasm Evaluation of *Glycine max* for Resistance to *Fusarium solani*, the Causal Organism of Sudden Death Syndrome. Plant Disease. 81:515–518

Hepperle, D. 2004. SeqAssem©: a sequence analysis tool contig assembler and trace data visualization tool or molecular sequences. Klein Raden: Sequantix

Huang, Y. H., and Hartman, G. L. 1998. Reaction of Selected Soybean Genotypes to Isolates of *Fusarium solani* f. sp. *glycines* and Their Culture Filtrates. Plant Disease. 82:999–1002

Jeewon, R. 2002. Phylogenetic relationships of *Pestalotiopsis* and allied genera inferred from ribosomal DNA sequences and morphological characters. Molecular Phylogenetics and Evolution. 25:378–392

Jin H., Hartman G. L., Nickell C. D., Widbolm J. M. 1996. Characterization and purification of a phytotoxin produced by *Fusarium solani*, the causal agent of soybean sudden death syndrome. Phytopathology 86:277–282

Kandel, Y. R., Bradley, C. A., Wise, K. A., Chilvers, M. I., Tenuta, A. U., Davis, V. M., et al. 2015. Effect of Glyphosate Application on Sudden Death Syndrome of Glyphosate-Resistant Soybean Under Field Conditions. Plant Disease. 99:347–354

Kumar, S., Stecher, G., Li, M., Knyaz, C., and Tamura, K. 2018. MEGA X: Molecular Evolutionary Genetics Analysis across Computing Platforms ed. Fabia Ursula Battistuzzi. Molecular Biology and Evolution. 35:1547–1549

Kumawat, G., Gupta, S., Ratnaparkhe, M. B., Maranna, S., and Satpute, G. K. 2016. QTLomics in Soybean: A Way Forward for Translational Genomics and Breeding. Front. Plant Sci. 7

Liu, Y. J., Whelen, S., and Hall, B. D. 1999. Phylogenetic relationships among ascomycetes: evidence from an RNA polymerse II subunit. Molecular Biology and Evolution. 16:1799–1808

Nalim, F. A., Samuels, G. J., Wijesundera, R. L., and Geiser, D. M. 2011. New species from the *Fusarium solani* species complex derived from perithecia and soil in the Old World tropics. Mycologia. 103:1302–1330

O'Donnell K. 2000. Molecular phylogeny of the *Nectria haematococca-Fusarium sola*ni species complex. Mycologia 92:919–938.

O'Donnell, K., Al-Hatmi, A. M. S., Aoki, T., Brankovics, B., Cano-Lira, J. F., Coleman, J. J., et al. 2020. No to *Neocosmospora* : Phylogenomic and Practical Reasons for Continued Inclusion of the *Fusarium solani* Species Complex in the Genus *Fusarium* ed. Aaron P. Mitchell. mSphere. 5:e00810-20

O'Donnell, K., Sink, S., Scandiani, M. M., Luque, A., Colletto, A., Biasoli, M., et al. 2010. Soybean Sudden Death Syndrome Species Diversity Within North and South America Revealed by Multilocus Genotyping. Phytopathology®. 100:58–71

O'Donnell, K., Sutton, D. A., Fothergill, A., McCarthy, D., Rinaldi, M. G., Brandt, M. E., et al. 2008. Molecular Phylogenetic Diversity, Multilocus Haplotype Nomenclature, and In Vitro Antifungal Resistance within the *Fusarium solani* Species Complex. J Clin Microbiol. 46:2477–2490

Promputtha, I., Jeewon, R., Lumyong, S., McKenzie, E. H. C., Hyde, K. D. 2005. Ribosomal DNA fingerprinting in the identification of non-sporulating endophytes from *Magnolia liliifera* (*Magnoliaceae*). Fungal Divers 20:167-186

Promputtha, I., Lumyong, S., Dhanasekaran, V., McKenzie, E. H. C., Hyde, K. D., and Jeewon, R. 2007. A Phylogenetic Evaluation of Whether Endophytes Become Saprotrophs at Host Senescence. Microb Ecol. 53:579–590

Pudake, R. N., Swaminathan, S., Sahu, B. B., Leandro, L. F., and Bhattacharyya, M. K. 2013. Investigation of the *Fusarium virguliforme* fvtox1 mutants revealed that the FvTox1 toxin is involved in foliar sudden death syndrome development in soybean. Curr Genet. 59:107–117

R Core Team. 2023. R: A Language and Environment for Statistical Computing. R Foundation for Statistical Computing, Vienna, Austria. https://www.R-project.org/

Roy, K. W. 1997. *Fusarium solani* on Soybean Roots: Nomenclature of the Causal Agent of Sudden Death Syndrome and Identity and Relevance of *F. solani* form B. Plant Disease. 81:259–266

Roy K. W., State M., Rupe J. C., Hershman D. E., Abney T. S. , Lafayette W. et al. 1997. Sudden death syndrome of soybean. Plant Dis 81:1100–1111

Rupe, J. C., Correll, J. C., Guerber, J. C., Becton, C. M., Gbur, Jr., E. E., Cummings, M. S., et al. 2001. Differentiation of the sudden death syndrome pathogen of soybean, *Fusarium solani* f.sp. *glycines*, from other isolates of *F. solani* based on cultural morphology, pathogenicity, and mitochondrial DNA restriction fragment length polymorphisms. Can. J. Bot. 79:829–835

Sabahi, F., Banihashemi, Z., Mirtalebi, M., Rep, M., and Cacciola, S. O. 2023. Molecular Variability of the *Fusarium solani* Species Complex Associated with Fusarium Wilt of Melon in Iran. Journal of Fungi. 9:486

Sandoval-Denis, M., and Crous, P. W. 2018. Removing chaos from confusion: assigning names to common human and animal pathogens in *Neocosmospora*. persoonia. 41:109–129

Sandoval-Denis, M., Lombard, L., and Crous, P. W. 2019. Back to the roots: a reappraisal of *Neocosmospora*. persoonia. 43:90–185

Scandiani, M. M., Carmona, M. A., Luque, A. G., Matos, K. D. S., Lenzi, L., Formento, Á. N., et al. 2012. Aislamiento, identificación y daños asociados al síndrome de la muerte súbita en el cultivo de soja en Argentina. Trop. plant pathol. 37:358–362

Scandiani, M., Ruberti, D., O'Donnell, K., Aoki, T., Pioli, R., Giorda, L., et al. 2004. Recent Outbreak of Soybean Sudden Death Syndrome Caused by *Fusarium virguliforme* and *F. tucumaniae* in Argentina. Plant Disease. 88:1044–1044

Schroers, H.-J., Samuels, G. J., Zhang, N., Short, D. P. G., Juba, J., and Geiser, D. M. 2016. Epitypification of *Fusisporium* (*Fusarium*) *solani* and its assignment to a common phylogenetic species in the *Fusarium solani* species complex. Mycologia. 108:806–819

Senanayake, I et al. 2020. Morphological approaches in studying fungi: collection, examination, isolation, sporulation and preservation. Mycosphere. 11:2678–2754

Spampinato, C. P., Scandiani, M. M., and Luque, A. G. 2021. Soybean sudden death syndrome: Fungal pathogenesis and plant response. Plant Pathology. 70:3–12

Sung, G.-H., Sung, J.-M., Hywel-Jones, N. L., and Spatafora, J. W. 2007. A multi-gene phylogeny of *Clavicipitaceae* (Ascomycota, Fungi): Identification of localized incongruence using a combinational bootstrap approach. Molecular Phylogenetics and Evolution. 44:1204–1223

Tewoldemedhin, Y. T., Lamprecht, S. C., Geldenhuys, J. J., and Kloppers, F. J. 2014. First Report of Soybean Sudden Death Syndrome Caused by *Fusarium virguliforme* in South Africa. Plant Disease. 98:569–569

Tewoldemedhin, Y. T., Lamprecht, S. C., Vaughan, M. M., Doehring, G., and O'Donnell, K. 2017. Soybean SDS in South Africa is Caused by *Fusarium brasiliense* and a Novel Undescribed *Fusarium* sp. Plant Disease. 101:150–157

Thompson, J. D., Higgins, D. G., and Gibson, T. J. 1994. CLUSTAL W: improving the sensitivity of progressive multiple sequence alignment through sequence weighting, position-specific gap penalties and weight matrix choice. Nucl Acids Res. 22:4673–4680

Wang, J., Sang, H., Jacobs, J. L., Oudman, K. A., Hanson, L. E., and Chilvers, M. I. 2019. Soybean Sudden Death Syndrome Causal Agent *Fusarium brasiliense* Present in Michigan. Plant Disease. 103:1234–1243

Xiang, Y., Scandiani, M. M., Herman, T. K., and Hartman, G. L. 2015. Optimizing Conditions of a Cell-Free Toxic Filtrate Stem Cutting Assay to Evaluate Soybean Genotype Responses to *Fusarium* Species that Cause Sudden Death Syndrome. Plant Disease. 99:502–507

Zhang, N., O'Donnell, K., Sutton, D. A., Nalim, F. A., Summerbell, R. C., Padhye, A. A., et al. 2006. Members of the *Fusarium solani* Species Complex That Cause Infections in Both Humans and Plants Are Common in the Environment. J Clin Microbiol. 44:2186–2190

CAPÍTULO 3 – EDIÇÃO GENÉTICA DE *Fusarium virguliforme* UTILIZANDO CRISPR/CAS9

1. INTRODUÇÃO

1.1 CRISPR

CRISPR (*Clustered Regularly Interspaced Short Palindromic Repeat*) diz respeito ao tipo de organização única de curtas e parcialmente repetidas sequências de DNA encontradas no genoma de procariotos. Em conjunto com a proteína associada Cas9, o sistema CRISPR/Cas9 atua como um método de imunidade adaptativa em procariotos, defendendo-os contra vírus e bacteriófagos (Hille e Charpentier, 2016). De acordo com a estrutura e função das proteínas-Cas, o sistema CRISPR/Cas pode ser dividido em Classe I (tipo I, III e IV) e Classe II (tipo II, V e VI) (Mohanraju et al., 2016). Sistemas do tipo I, II e V reconhecem e clivam DNA, tipo VI pode editar RNA, tipo III edita tanto DNA quanto RNA e o efeito do sistema tipo IV em DNA ou RNA ainda não é conhecido (Wang et. al, 2019). Devido a sua estrutura relativamente simples, o sistema CRISPR/Cas9 (tipo II) é bem estudado e extensivamente utilizado na engenharia genética (Liu et al., 2020).

O RNA-guia e a proteína associada Cas9 são dois elementos fundamentais do sistema CRISPR/Cas9. A proteína Cas9, extraída de *Streptococcus pyogenes*, foi a primeira a ser utilizada em edição genômica. Esta proteína tem 1368 aminoácidos, é uma endonuclease de DNA multi-domínios que é responsável por clivar o DNA-alvo (Mei et al., 2016). A proteína Cas9 possui duas regiões conhecidas como lóbulo de reconhecimento (REC) e lóbulo da nuclease (NUC). O lóbulo REC é composto pelos domínios REC1 e REC2 que são responsáveis pela ligação com o RNA-guia, enquanto o lóbulo NUC é composto pelos domínios RuvC, HNH e PAM (protospacer adjacent motif). Os domínios RuvC e HNH são utilizados para clivar cada fita simples do DNA enquanto o domínio PAM confere especificidade e é responsável pelo início da ligação com o DNA alvo (Nishimasu et al., 2014). O RNA-guia é dividido em dois componentes, crRNA (CRISPR RNA) e tracrRNA (trans-activating CRISPR RNA). O crRNA possui 18-20 pares de base que especificam o DNA alvo através do pareamento com a sequência-alvo. O tracrRNA é um longo trecho em loop que funciona como base para a ligação da nuclease Cas9. Em procariotos, o RNA-guia é utilizado para identificar DNA viral, porém, quando usado como uma ferramenta de edição gênica, ele pode ser sinteticamente projetado através da combinação do crRNA e tracrRNA formando um único RNA-guia (sgRNA) específico para qualquer sequência de um gene de interesse de edição (Mei et al., 2016).

O mecanismo de edição gênica do CRISPR/Ca9 pode ser dividido em 3 etapas: reconhecimento, clivagem e reparo (Shao et al., 2016). O sgRNA direciona a Cas9 e reconhece a região alvo da sequência do gene de interesse através do componente complementar 5'crRNA. Sem o sgRNA, a proteína Cas9 permanece inativa. A nuclease da Cas9 produz double-stranded breaks (DBS) na localização 3 pares de base upstream da PAM (Ceasar et al., 2016) que é um fragmento conservado de DNA com 2-5 pares de base downstream do local de clivagem. A Cas9 reconhece a sequência PAM 5'-NGG-3' e em seguida induz a formação do híbrido RNA-DNA, seguido pela clivagem do DNA. O domínio HNH cliva a fita complementar enquanto o domínio RuvC cliva a fita não-complementar do DNA alvo gerando a DBS. Finalmente, a DBS é reparada pelo maquinário celular do hospedeiro (Mei et al., 2016; Jiang e Doudna., 2017).

Os dois métodos de reparo da DBS são NHEJ (non-homologous end joining) e HDR (homology-directed repair) (Liu et al., 2019). NHEJ facilita o reparo da DBS através da junção dos fragmentos do DNA por um processo enzimático na ausência de DNA homólogo externo. É um sistema de reparo eficiente, porém, é suscetível a erros que podem resultar em inserções ou deleções aleatórias no local de clivagem que causam mutações (Yang et al., 2020). Em contraste, o HDR é um método altamente preciso que necessita do template do DNA homólogo que contém uma sequência de interesse. O HDR executa a inserção ou substituição exata do gene ao adicionar a sequência doadora do DNA-template no local da DBS (Liu et al., 2019; Yang et al., 2020).

1.2. Genes FvTox1 e FvNIS1 de *Fusarium virguliforme*

FvTox1 é um gene único presente no genoma de *F. virguliforme*, identificado por Brar et al. (2011) e que codifica uma proteína ácida de 13,5 kDa. Esta proteína é uma fitotoxina considerada como um fator de patogenicidade e virulência de *F. virguliforme.* Seu mecanismo de ação ainda não está totalmente elucidado, porém, sabemos que ela é capaz de reduzir o conteúdo de clorofila das folhas, contribuindo para o desenvolvimento da clorose foliar da síndrome da morte súbita da soja (Brar et al., 2011; Pudake et al., 2013).

O gene FvNIS1 identificado por Chang et al. (2016) também em *F. virguliforme* codifica um proteína ortóloga à proteína secretada NIS1 de *Colletotrichum obiculare* (Yoshino et al. 2012). Esta proteína também está relacionada com o desenvolvimento da clorose e necrose internerval foliar características da doença, sendo que folhas com sintomas mais severos podem também apresentar enrolamento foliar e serem facilmente destacadas dos pecíolos (Chang et al., 2016).

2. OBJETIVO

O objetivo deste projeto foi criar vetores contendo fragmento da sequência individual e conjunta dos genes FvTox1 e FvNIS1 a serem usadas no silenciamento genético através do sistema CRISPR/Cas9 para estudar a sua influência no desenvolvimento dos sintomas foliares da síndrome da morte súbita da soja.

3. MATERIAL E MÉTODOS

3.1. Criação dos vetores contendo Tox1 e NIS1

3.1.1. Obtenção das cassetes individuais Tox1 e NIS1

Com auxílio da ferramenta CHOPCHOP (https://chopchop.cbu.uib.no/) a região-alvo dos genes FvTox1 (JF440964.1) e FvNIS1 (GBJV01011406.1) foram definidas baseado no conteúdo de GC e eficiência. O template PWC1 que continha o Gln-tRNA promoter + target RNA + scaffold (Figura 5) foi utilizado como backbone na criação da sequência de interesse que foram sintetizadas através da tecnologia gBlock™ pela empresa IDT (Coralville, IA, EUA).

As cassetes de cada gene foram individualmente amplificadas através de PCR com o mix Q5® High-Fidelity DNA Polymerase (New England Biolabs®) para obter um volume final de 150 µL. Os primers gRNA_F e gRNA_R (Tabela 3) (244 bp) foram utilizados na reação. As condições de amplificação foram: 98°C – 1 min, 35 ciclos 98°C – 10s, 58°C – 30s, 72°C – 15s, 72°C – 2 min, 16°C – 5 min. Após a confirmação do resultado em gel de agarose 1% corado com GelRed® (Biotium, EUA) e visualização no transiluminador GelDoc-ItTS52 Imager (Analytik Jena US, Alemanha), os fragmentos foram purificados de acordo com as instruções do fabricante utilizando o Monarch DNA and PCR clean up kit (New England Biolabs®). A concentração e qualidade dos fragmentos foram determinadas utilizando NanoDrop™ 2000 (Thermo Fisher Scientific, EUA).

Os fragmentos foram digeridos pelas enzimas HindIII e XbaI durante 12 h a 16°C numa reação com 21 µL do template, 1 µL HindIII, 1 µL XbaI, 5 µL buffer r2.1 (New England Biolabs®) e 22 µL de dH_2O. Após a digestão, os fragmentos foram purificados utilizando o Monarch DNA and PCR clean up kit (New England Biolabs®) de acordo com as instruções do fabricante. A concentração e qualidade dos fragmentos foram determinadas utilizando NanoDrop™ 2000 (Thermo Fisher Scientific, EUA).

3.1.2. Vetor

O vetor pUC19 (Figura 6) foi utilizado neste experimento. A digestão do vetor foi realizada com as enzimas HindIII e XbaI nas mesmas condições de digestão dos fragmentos de interesse.

3.1.3. Ligação T4 entre vetor e cassetes individuais

A ligação entre pUC19 + FvTox1 e pUC19 + FvNIS1 foi feita através da enzima T4 DNA ligase. As reações individuais de 10 µL de volume final contendo 1µL buffer; 1 µL enzima T4; 1 µL vetor e 7 µL fragmento digerido foram incubadas por 6h em temperatura ambiente.

3.1.4. Preparo de células competentes de *E. coli*

E. coli foi cultivado por 12h em meio YENB líquido (0,75% bacto yeast extract e 0,8% bacto nutrient broth). Em seguida, 1 L de meio YENB líquido foi inoculado com 5 – 10 mL da cultura fresca de *E. coli* e incubado a 37°C sob agitação. A coleta das células foi feita quando a OD_{600} atingiu 0,5 – 0,9. Os frascos foram incubados por 5 min em gelo, centrifugado a 4000 g por 10 min a 4°C e o sobrenadante foi descartado. O pellet foi lavado em 100 mL de água destilada estéril gelada, novamente centrifugado a 4000 g por 10 min a 4°C, seguido pelo descarte do sobrenadante. O processo de lavagem do pellet foi repetido duas vezes. Em seguida, foi feita a ressuspensão em 20 mL de solução de glicerol 10% gelada. As amostras foram centrifugadas a 4.000 g por 10 min a 4°C. O sobrenadante foi descartado e a ressuspensão final das células foi feita em 2 – 3 mL da solução de glicerol 10% gelada. As células competentes foram armazenadas a -70°C para uso futuro.

3.1.5. Transformação de *E. coli*

A transformação de *E. coli* para a inserção dos vetores de interesse foi feita através da eletroporação. 40 µL de células competentes de *E. coli* foram misturadas com 5 µL do produto da ligação T4. 40 µL dessa mistura foram transferidos para uma cubeta de vidro adequada para a eletroporação e inserida no equipamento. Após a transformação, as células foram misturadas com 1 mL de meio Luria Bertani líquido (LB; 8 g triptona; 5 g extrato de levedura; 10 g NaCl; 1 L dH_2O), transferidas para microtubo e incubado sob agitação (190 rpm) por 1h a 37°C. Os microtubos foram centrifugados a 12.000 rpm por 30s. 400 µL do sobrenadante foi descartado e as células foram ressuspendidas no restante do líquido. 100 µL foram transferidos para placas de Petri contendo meio LB suplementado com ampicilina (1 mg/mL), X-Gal (200 µg/mL) e IPTG (1 mM), espalhados com alça de Drigaslki e incubadas por 12 h a 37°C.

3.1.6. Seleção de transformantes

Foram aleatoriamente selecionadas 10 colônias bacterianas de cor azul (indício da inserção do vetor) para a PCR de confirmação da inserção dos fragmentos de interesse. O vetor pUC19 foi utilizado como controle negativo. Os primers utilizados foram gRNA_F e P2.Tox1_R para o gene FvTox1 e gRNA_F e P2.NIS1_R para o gene FvNIS1 (Tabela 3) cujo produto de amplificação esperado de ambos é de 130 bp. O mix *Taq* DNA Polymerase with

Standard *Taq* Buffer (New England Biolabs®) foi utilizado nas seguintes condições de amplificação: 95°C – 10 min, 30 ciclos 95°C – 30s, 58°C – 30s, 72°C – 30s, 72°C – 2 min e 16°C – hold. Após a conferência do resultado em gel de agarose 1% corado com GelRed® (Biotium, EUA) e visualização no transiluminador GelDoc-ItTS52 Imager (Analytik Jena US, Alemanha), transformantes positivos foram preparados para o sequenciamento.

3.1.7. Obtenção do vetor para sequenciamento

Dois possíveis transformantes de cada vetor foram selecionados para o sequenciamento (Figura 10 A e B). Os transformantes foram cultivados por 12h a 37°C com agitação (190 rpm) em 2 mL de meio LB líquido suplementado com 100 mg/mL de ampicilina. Os plasmídeos foram extraídos com o kit PureLink™ Quick Plasmid miniprep (Invitrogen, Thermo Fisher Scientific, EUA) de acordo com as instruções do fabricante. A concentração do material genético foi determinada utilizando NanoDrop™ 2000 (Thermo Fisher Scientific, EUA).

Após a diluição para a concentração final de 10 ng/µL do material genético, foi realizada a PCR utilizando os primers gRNA_F e gRNA_R (Tabela 3) para confirmar a presença completa da cassete de interesse. O mix *Taq* DNA Polymerase with Standard *Taq* Buffer (New England Biolabs®) foi utilizado nas seguintes condições de amplificação: 95°C – 1 min, 30 ciclos 95°C – 30s, 58°C – 30s, 72°C – 30s, 72°C – 2 min e 16°C – 5 min. A confirmação do resultado foi feita em gel de agarose 1% corado com GelRed® (Biotium, EUA) visualizado no transiluminador GelDoc-ItTS52 Imager (Analytik Jena US, Alemanha).

Os 6 possíveis transformantes foram novamente cultivados em meio LB líquido e passaram pelo processo de extração do plasmídeo conforme descrito acima. Então, os plasmídeos contendo as cassetes individuais extraídos foram digeridos pelas enzimas HindIII e XbaI por 1h a 37°C. A reação de digestão foi realizada para um volume final de 90 µL contendo 9 µL HindIII, 9 µL XbaI, 18 µL buffer r2.1 (New England Biolabs®) e 54 µL dH_2O. Em seguida, foi feita a confirmação da digestão em gel de agarose 2% corado com GelRed® (Biotium, EUA) e visualização no transiluminador GelDoc-ItTS52 Imager (Analytik Jena US, Alemanha).

3.1.8. Sequenciamento

O sequenciamento completo dos plasmídeos digeridos foi realizado pela empresa Genewiz by Azenta Life Science (South Plainfield, NJ, EUA) utilizando o primer M13R (Tabela 3). A confirmação da inserção das cassetes individuais foi feita utilizando o SnapGene Viewer (SnapGene® software).

3.2 Criação do vetor contendo Tox1 + NIS1

3.2.1. Obtenção do vetor e cassetes de interesse

E. coli contendo individualmente os plasmídeos Tox1#4 e NIS1#1 foi cultivada por 12h a 37°C com agitação (190 rpm) em 3 mL de meio LB líquido suplementado com 100 mg/mL de ampicilina. Os plasmídeos foram extraídos com o kit PureLink™ Quick Plasmid miniprep (Invitrogen, Thermo Fisher Scientific, EUA) de acordo com as instruções do fabricante e a concentração do material genético foi determinada utilizando NanoDrop™ 2000 (Thermo Fisher Scientific, EUA).

A PCR utilizando as cassetes Tox1 e NIS1 sintetizadas pela IDT foi repetida nas mesmas condições descritas em 2.1.1. A purificação dos fragmentos foi realizada de acordo com as instruções do fabricante utilizando o Monarch DNA and PCR clean up kit (New England Biolabs®). A concentração e qualidade dos fragmentos foram determinadas utilizando NanoDrop™ 2000 (Thermo Fisher Scientific, EUA).

3.2.1.1. Tox1#4 + NIS1

O plasmídeo Tox1#4 e a cassete NIS1 foram digeridos com as enzimas EcoRI e BamHI por 12h a 16°C. A reação de digestão dos plasmídeo teve volume final de 100 µL contendo: 25 µL plasmídeo, 10 µL buffer rCutSmart™ (New England Biolabs®), 2 µL EcoRI, 2 µL BamHI e 61 µL dH_2O. A reação de digestão da cassete teve volume final de 50 µL contendo: 21 µL fragmento, 5 µL buffer rCutSmart™ (New England Biolabs®), 1 µL EcoRI, 1 µL BamHI e 22 µL dH_2O. Após a digestão, o plasmídeo foi purificado com o kit PureLink™ Quick Plasmid miniprep (Invitrogen, Thermo Fisher Scientific, EUA) enquanto o fragmento digerido foi purificado utilizando o Monarch DNA and PCR clean up kit (New England Biolabs®) de acordo com as instruções dos fabricantes.

3.2.1.2. NIS1#1 + Tox1

O plasmídeo NIS1#1 e a cassete Tox1 também foram digeridos com as enzimas EcoRI e BamHI por 12h a 16°C. A reação de digestão dos plasmídeo teve volume final de 100 µL contendo: 15 µL plasmídeo, 10 µL buffer rCutSmart™ (New England Biolabs®), 2 µL EcoRI, 2 µL BamHI e 71 µL dH_2O. A reação de digestão da cassete teve volume final de 50 µL contendo: 21 µL fragmento, 5 µL buffer rCutSmart™ (New England Biolabs®), 1 µL EcoRI, 1 µL BamHI e 22 µL dH_2O. Após a digestão, o plasmídeo foi purificado com o kit PureLink™ Quick Plasmid miniprep (Invitrogen, Thermo Fisher Scientific, EUA) enquanto o fragmento digerido foi purificado utilizando o Monarch DNA and PCR clean up kit (New England Biolabs®) de acordo com as instruções dos fabricantes.

3.2.2. Ligação T4 e transformação

As ligações de Tox1#4 + NIS1 e NIS1#1 + Tox1 foram realizadas com a enzima T4 DNA ligase em reações individuais contendo 1µL buffer; 1 µL enzima T4; 1 µL vetor e 7 µL fragmento digerido incubada por 12h em temperatura ambiente. Após a ligação, a transformação de *E. coli* foi realizada da mesma maneira descrita em 2.1.5.

3.2.3. Seleção de transformantes

Foram selecionadas todas as colônias oriundas das transformações de Tox1#4 + NIS1 e NIS1#1 + Tox1 que apresentavam coloração azul. A PCR de confirmação da inserção do fragmento de interesse foi realizada utilizando os primers P1.Tox1_F e P1.NIS1_F, cujo produto esperado é de 282 bp (Tabela 3). Os vetores pUC19 contendo o plasmídeo Tox1#4 e NIS1#1 foram utilizados como controle negativo. As condições de amplificação e confirmação do resultado foram as mesmas descritas em 2.1.6.

3.2.4. Obtenção do vetor para sequenciamento

Dois possíveis transformantes de Tox1#4 + NIS1 e NIS1#1 + Tox1 foram cultivados em 3 mL de meio LB líquido suplementado com 100 mg/mL de ampicilina por 12h a 37°C com agitação (190 rpm). Os plasmídeos foram extraídos com o kit PureLink™ Quick Plasmid miniprep (Invitrogen, Thermo Fisher Scientific, EUA) de acordo com as instruções do fabricante. A concentração do material genético foi determinada utilizando NanoDrop™ 2000 (Thermo Fisher Scientific, EUA).

O material genético foi diluído para a concentração final de 10 ng/uL. Foi realizada uma PCR com os primers M13F e M13R (Tabela 3) (420 bp) para confirmar a presença da cassete dupla. O mix *Taq* DNA Polymerase with Standard *Taq* Buffer (New England Biolabs®) foi utilizado nas seguintes condições de amplificação: 95°C - 2 min, 35 ciclos 95°C - 45s, 58°C - 45s, 72°C - 30s, 72°C - 2 min e 4°C - hold. A confirmação do resultado foi feita em gel de agarose 1% corado com GelRed® (Biotium, EUA) e visualizado no transiluminador GelDoc-ItTS52 Imager (Analytik Jena US, Alemanha).

Os possíveis transformantes foram novamente cultivados em meio LB líquido e passaram pelo processo de extração do plasmídeo conforme descrito acima. Os plasmídeos foram digeridos com a enzima HindIII por 1h a 37°C numa reação de 20 µL de volume final contendo 5 µL plasmídeo, 1 µL HindIII, 2 µL buffer 2 (New England Biolabs®) e 13 µL dH_2O. O resultado da digestão foi confirmado em gel de agarose 2% corado com GelRed® (Biotium, EUA) e visualizado no transiluminador GelDoc-ItTS52 Imager (Analytik Jena US, Alemanha).

3.2.5. Sequenciamento

O sequenciamento completo dos plasmídeos foi feito pela empresa Genewiz by Azenta Life Science (South Plainfield, NJ, EUA) utilizando os primers M13F e M13R. A confirmação da inserção das cassetes individuais foi feita utilizando o SnapGene Viewer (SnapGene® software).

3.3. Criação do vetor contendo Cas9 + hyg-b (higromicina-b)

3.3.1. Obtenção do vetor e fragmento de interesse

O vetor XuLab Cas9 backbone (Figura 9) que contém o gene Cas9 e plasmídeo HYG/B que continha o gene hyg-b foram utilizados nesse experimento. Ambos foram cultivados em 3 mL de meio LB líquido suplementado com 100 mg/mL de ampicilina por 12h a 37°C com agitação (190 rpm). Os plasmídeos foram extraídos com o kit PureLink™ Quick Plasmid miniprep (Invitrogen, Thermo Fisher Scientific, EUA) de acordo com as instruções do fabricante. A concentração do material genético foi determinada utilizando NanoDrop™ 2000 (Thermo Fisher Scientific, EUA).

Os primers HYG/F e HYG/R (Tabela 3) (1600 bp) foram utilizados na reação de PCR de 150 µL de volume final para amplificar o gene hyg-b do plasmídeo HYG/B. O mix Q5® High-Fidelity DNA Polymerase (New England Biolabs®) foi utilizado nas seguintes condições de amplificação: 98°C – 1 min, 30 ciclos 98°C – 10 s, 60°C – 30 s, 72°C – 1 min, 72°C – 2 min, 16°C – 5 min. O resultado foi confirmado em gel de agarose 0,8% corado com GelRed® (Biotium, EUA) visualizado no transiluminador GelDoc-ItTS52 Imager (Analytik Jena US, Alemanha).

O fragmento hyg-b amplificado foi purificado utilizando o Monarch DNA and PCR clean up kit (New England Biolabs®) de acordo com as instruções do fabricante. A concentração e qualidade dos produtos foram determinadas utilizando NanoDrop™ 2000 (Thermo Fisher Scientific, EUA). A digestão foi feita com as enzimas XbaI e EcoRI-HF por 12h a 16°C em reações de 150 µL de volume final. A reação de digestão do vetor XuLab Cas9 backbone continha 3 µL XbaI, 3 µL EcoRI-HF, 3 µL plasmídeo, 15 µL buffer rCutSmart™ (New England Biolabs®) e 126 µL dH_2O. Já a reação de digestão do fragmento hyg-b continha 28 µL fragmento, 3 µL XbaI, 3 µL EcoRI-HF, 15 µL buffer rCutSmart™ (New England Biolabs®) e 101 µL dH_2O.

Após a digestão, o vetor XuLab Cas9 backbone foi purificado utilizando o kit PureLink™ Quick Plasmid miniprep (Invitrogen, Thermo Fisher Scientific, EUA) e o fragmento hyg-b com o Monarch DNA and PCR clean up kit (New England Biolabs®) de acordo com as instruções

dos fabricantes. A concentração e qualidade dos produtos digeridos foram determinadas utilizando NanoDrop™ 2000 (Thermo Fisher Scientific, EUA).

3.3.2. Ligação T4 e transformação

A ligações do plasmídeo XuLab Cas9 backbone e do fragmento hyg-b foi realizada com a enzima T4 DNA ligase numa reação contendo 1 µL vetor, 2 µL fragmento, 1 µL buffer, 1 µL enzima T4 e 5 µL dH_2O incubada por 12h a 16°C. A enzima T4 foi inativada através da incubação a 65°C por 15 min. Após a ligação, a transformação de *E. coli* foi realizada da mesma maneira descrita em 2.1.5.

3.3.3. Seleção de transformantes

As colônias de cor azul foram selecionadas para a PCR de confirmação de inserção do gene hyg-b. Os primers HYG/F e HYG/R foram utilizados na reação de PCR realizada com o mix *Taq* DNA Polymerase with Standard *Taq* Buffer (New England Biolabs®) nas seguintes condições de amplificação: 95°C – 10 min, 30 ciclos 95°C – 30s, 68°C – 30s, 72°C – 90s, 72°C – 5 min, 4°C – hold. O plasmídeo HYG/B foi utilizado como controle negativo. A confirmação do resultado foi feita em gel de agarose 1% corado com GelRed® (Biotium, EUA) e visualizado no transiluminador GelDoc-ItTS52 Imager (Analytik Jena US, Alemanha).

3.3.4. Obtenção do vetor para sequenciamento

Dois possíveis transformantes de XuLab Cas9 backbone + hyg-b (Figura 10 C) foram cultivados em 3 mL de meio LB líquido suplementado com 100 mg/mL de ampicilina por 12h a 37°C com agitação (190 rpm). Os plasmídeos foram extraídos com o kit PureLink™ Quick Plasmid miniprep (Invitrogen, Thermo Fisher Scientific, EUA) de acordo com as instruções do fabricante. A concentração do material genético foi determinada utilizando NanoDrop™ 2000 (Thermo Fisher Scientific, EUA).

3.3.5. Sequenciamento

O sequenciamento completo dos plasmídeos utilizando os primers HYG/F e HYG/R foi realizado pela empresa Genewiz by Azenta Life Science (South Plainfield, NJ, EUA). A confirmação da inserção de hyg-b foi feita utilizando o SnapGene Viewer (SnapGene® software).

3.4. Obtenção de protoplastos de *F. virguliforme*

5 mL de dH_2O foram adicionados a placas de *F. virguliforme* (NRRL 34551; Mont-1) (Figura 10 D) cultivadas em meio MA 2% 15 dias a 25°C com 12h de fotoperíodo. Foi feita a raspagem da placa, filtragem dos esporos em 2 camadas de gaze e ajuste da concentração de esporos para 1×10^7 conídios/mL. 50 mL de meio MA 2% líquido foram inoculados com a

suspensão de esporos e incubado por 3 dias a 28°C com agitação (130 rpm). Após a incubação, o micélio foi filtrado em miracloth e 1 – 1,5 g de micélio fresco foi transferido para um frasco estéril contendo 30 mL da solução de protoplastização (30 mL 1,2M KCl; 750 mg driselase; 1,5 mg quitinase; 150 mg enzima lítica. A solução foi agitada por 30 min e esterilizada através de filtragem em filtro de poro 0,45 µm). O frasco foi incubado a 30°C com agitação (75 rpm) por 3 - 5 h. A concentração de protoplasto foi conferida a cada hora e os mesmos foram filtrados em filtro Nylon com malha de 30 µm, centrifugados a 3000 g a 4°C por 5 min. O sobrenadante foi descartado e os protoplastos foram ressuspendidos em 10 mL de solução STC gelada (1,2 M sorbitol; 10 mM $CaCl_2$ e 10 mM Tris-HCl, pH 7,5). A centrifugação e a ressuspensão em STC gelado foi repetida duas vezes, sendo que na última, os protoplastos foram ressuspensos em apenas 400 µL de STC gelado + 30,1 µL DMSO (concentração final 7%). Os protoplastos foram armazenados a -80°C para uso futuro (Figura 10 E – I) (Roth e Chilvers 2019, com modificações).

3.5. Transformação de *F. virguliforme*

Os protoplastos que estavam armazenados a -80°C foram descongelados em gelo e centrifugados a 3000 g a 4°C por 4 min. O sobrenadante foi descartado e o pellet ressuspendido em 200 µL de STC gelado. A etapa de centrifugação e ressuspensão foi repetida duas vezes. A reação de transformação foi composta por 20 µL de protoplastos em solução STC, 5 µg do plasmídeo linearizado e 50 µL de solução PEG-8000 30% (para 25 mL: 7,5 g PEG-8000; 10 mM Tris-HCL pH 8,0 e 50 mM $CaCl_2$. A solução foi agitada por 30 min e esterilizada através de filtragem em filtro de poro 0,45 µm). O tubo com a reação de transformação foi invertido gentilmente 3 vezes e incubado em gelo por 1h. 2 mL de solução PEG-8000 30% e 4 mL de STC também foram incubados em gelo por 1h. Após a incubação, a reação de transformação foi transferida para o tubo contendo a solução PEG-8000 30% e incubada em gelo por 15 min. Em seguida, os 4 mL de STC gelado foram adicionados ao tubo que então foi gentilmente misturado por inversão 3 vezes. Os protoplastos foram imediatamente transferidos para o meio de regeneração que estava a 45°C (39 g BDA; 271 g sacarose, concentração final 0,8 M e 1 L H_2O). O meio suplementado com os protoplastos foi gentilmente misturado e transferido para placas de Petri. Após a incubação das placas por 24h a 25°C com fotoperíodo foi adicionado 15 mL do meio de regeneração suplementado com 200 µg/mL de higromicina B e as placas foram novamente incubadas a 25°C com fotoperíodo. O monitoramento de transformadores foi feito pelo período de 7 a 10 dias (Roth e Chilvers 2019).

4. RESULTADOS

Os vetores Tox1#4 (Figura 7A) e NIS1#1 (Figura 7B), que contém, respectivamente, a cassete Tox1 e NIS1, foram criados com sucesso com esta metodologia. A tentativa de criar um único vetor contendo as duas cassetes de interesse não foi bem sucedida. Após o sequenciamento, confirmamos que apesar do vetor Tox1+NIS1#9 (Figura 8) conter as duas regiões alvo dos genes de interesse, a cassete NIS1 não foi inserida por completo no momento da transformação. Por fim, criamos com sucesso o vetor contendo o gene Cas9 + hyg-b que foi selecionado para a etapa de transformação. A obtenção de protoplastos de *F. virguliforme* foi realizada, entretanto, a transformação do isolado não foi bem sucedida.

São necessários ajustes no processo de criação do vetor com a cassete dupla de Tox1 e NIS1 para garantir a completa inserção das sequências. Também é necessário a inserção dos genes Cas9 e hyg-b nos vetores individuais (Tox1#4 e NIS1#1) e duplo (Tox1+NIS1) antes da transformação de *F. virguliforme*. Finalmente, experimentos com plantas de soja inoculadas com os mutantes após o silenciamento genético devem ser executados para estudar o efeito das toxinas no desenvolvimento da clorose e necrose foliar característica da síndrome da morte súbita da soja.

REFERÊNCIAS

BRAR, H. K.; SWAMINATHAN, S.; BHATTACHARYYA, M. K. The *Fusarium virguliforme* Toxin FvTox1 Causes Foliar Sudden Death Syndrome-Like Symptoms in Soybean. **Molecular Plant-Microbe Interactions®**, v. 24, n. 10, p. 1179–1188, out. 2011.

CEASAR, S. A. et al. Insert, remove or replace: A highly advanced genome editing system using CRISPR/Cas9. **Biochimica Et Biophysica Acta**, v. 1863, n. 9, p. 2333–2344, set. 2016.

CHANG, H.-X. et al. Identification of Multiple Phytotoxins Produced by *Fusarium virguliforme* Including a Phytotoxic Effector (FvNIS1) Associated With Sudden Death Syndrome Foliar Symptoms. **Molecular Plant-Microbe Interactions®**, v. 29, n. 2, p. 96–108, fev. 2016.

HILLE, F.; CHARPENTIER, E. CRISPR-Cas: biology, mechanisms and relevance. **Philosophical Transactions of the Royal Society of London. Series B, Biological Sciences**, v. 371, n. 1707, p. 20150496, 5 nov. 2016.

JIANG, F.; DOUDNA, J. A. CRISPR-Cas9 Structures and Mechanisms. **Annual Review of Biophysics**, v. 46, p. 505–529, 22 maio 2017.

LIU, M. et al. Methodologies for Improving HDR Efficiency. **Frontiers in Genetics**, v. 9, 7 jan. 2019.

LIU, Z. et al. Application of different types of CRISPR/Cas-based systems in bacteria. **Microbial Cell Factories**, v. 19, n. 1, p. 172, 3 set. 2020.

MEI, Y. et al. Recent Progress in CRISPR/Cas9 Technology. **Journal of Genetics and Genomics**, v. 43, n. 2, p. 63–75, 20 fev. 2016.

MOHANRAJU, P. et al. Diverse evolutionary roots and mechanistic variations of the CRISPR-Cas systems. **Science**, v. 353, n. 6299, p. aad5147, 5 ago. 2016.

NISHIMASU, H. et al. Crystal structure of Cas9 in complex with guide RNA and target DNA. **Cell**, v. 156, n. 5, p. 935–949, 27 fev. 2014.

PUDAKE, R. N. et al. Investigation of the *Fusarium virguliforme* FvTox1 mutants revealed that the FvTox1 toxin is involved in foliar sudden death syndrome development in soybean. **Current Genetics**, v. 59, n. 3, p. 107–117, 1 ago. 2013.

ROTH, M. G.; CHILVERS, M. I. A protoplast generation and transformation method for soybean sudden death syndrome causal agents *Fusarium virguliforme* and *F. brasiliense*. **Fungal Biology and Biotechnology**, v. 6, n. 1, p. 7, 15 maio 2019.

SnapGene® software (from Dotmatics; available at snapgene.com)

SHAO, M.; XU, T.-R.; CHEN, C.-S. The big bang of genome editing technology: development and application of the CRISPR/Cas9 system in disease animal models. **Zoological Research**, v. 37, n. 4, p. 191–204, 18 jul. 2016.

WANG, F. et al. Advances in CRISPR-Cas systems for RNA targeting, tracking and editing. **Biotechnology Advances**, v. 37, n. 5, p. 708–729, set. 2019.

YANG, H. et al. Methods Favoring Homology-Directed Repair Choice in Response to CRISPR/Cas9 Induced-Double Strand Breaks. **International Journal of Molecular Sciences**, v. 21, n. 18, p. 6461, 4 set. 2020.

CAPÍTULO 4 - MODIFICAÇÃO GENÉTICA DE *Fusarium virguliforme* UTILIZANDO *Agrobacterium tumefaciens* MEDIATED TRANSFORMATION (ATMT)

1. INTRODUÇÃO

A transformação mediada por *Agrobacterium tumefaciens* (ATMT) é uma técnica para a inserção de DNA em diferentes hospedeiros que já foi aplicada com sucesso a mais de 125 espécies de fungos (Frandsen 2011). Para algumas, ATMT se tornou a técnica mais fácil ou a única disponível para esse tipo de introdução. Em outras, é vista como uma poderosa ferramenta de edição e manipulação genética para fins biotecnológicos (Idnurm et al., 2017).

A maioria dos membros do gênero *Agrobacterium* são bactérias que vivem no solo de forma saprofítica, porém, algumas são fitopatogênicas, como é o caso de *A. tumefaciens* que causa galha da coroa. De uma forma simplificada, o processo de transferência de DNA ocorre da seguinte maneira: o DNA de transferência (T-DNA) está localizado no plasmídeo indutor de tumor (Ti) de > 200 kb, que também contém os genes de virulência. Antes da transferência, o T-DNA é liberado do plasmídeo Ti por endonucleases que então entra na célula hospedeira. Em seguida, esse T-DNA é direcionado ao núcleo onde se integra ao genoma do hospedeiro garantindo replicação estável (Frandsen 2011).

Quando comparada a outras técnicas de transformação genética, a ATMT apresenta várias vantagens. Uma das principais, é a flexibilidade em escolher o material inicial para transformação (protoplasto, hifas, esporos ou micélio) (Liu et al., 2010). Também apresenta uma alta taxa de eficiência de transformação, alta taxa de inserção de cópia única e fácil identificação do T-DNA (Betts etl., 2007). E, ainda pode também ser utilizada em abordagem de genética-reversa para deleção ou interrupção de genes específicos (Idnurm et al., 2017).

Desde 2001, ATMT já foi relatada na transformação de várias espécies de *Fusarium*, sendo exemplos: *F. culmorum*, *F. graminearum* e *F. pseudograminearum* (Malz et al., 2005), *F. verticillioides* (Visentin et al., 2012), *F. virguliforme* (Pudake et al., 2013), *F. avenaceum* (Sørensen et al., 2014) e *F. oxysporum* (Dong e Wang 2022).

2. OBJETIVO

O objetivo deste trabalho foi criar mutantes de *F. virguliforme* contendo o gene eGFP para estudos sobre o processo de colonização de hospedeiro.

3. MATERIAL E MÉTODOS

3.1. Material biológico

O isolado NRRL 34551 de *F. virguliforme* (Figura 11 A) e a cepa SK1044 de *Agrobacterium tumefaciens* (Figura 11 B) foram utilizados na transformação. SK1044 tem uma

construção eGFP sob o controle do promotor trpC de *Aspergillus nidulans* no vetor binário T-DNA pBHt2. O vetor contém um T-DNA abrigando a resistência à higromicina-B (HYG/B) na estrutura do pCAMBIA1300 (Mullins et al., 2001).

3.2. Transformação

A cepa de *A. tumefaciens* foi cultivada em placa de Petri com meio LB suplementado com canamicina (50 mg/mL) por 2 dias a 28°C. Uma colônia isolada foi transferida para 5 mL de meio mínimo (MM; 10 mL de tampão K pH 7; 20 mL de tampão M-N; 1 mL de 1% $CaCl_2.H_2O$ (p/v); 10 mL de 20% de glicose (p/v); 10 mL de 0,01% $FeSO_4.7H_2O$ (p/v); 5 mL de elementos de esporos (100 mg/mL de $ZnSO_4.7H_2O$, $CuSO_4.5H_2O$, H_3BO_3, $MnSO_4.H_2O$ e $Na_2MoO_4.2H_2O$); 2,5 mL de 20% NH_4NO_3 (p/v); 1 L de dH_2O estéril) suplementado com canamicina (50 mg/mL) e incubado sob agitação (150 rpm) por 2 dias a 28°C (Figura 11 C). 200 µL da cultura em MM foi transferida para 5 mL de meio de indução (IM; 0,8 mL 1,25 M K-tampão pH 4,9; 20 mL M-N tampão; 1 mL 1% $CaCl_2.H_2O$ (p/v); 10 mL 0,01% $FeSO_4.7H_2O$ (p/v); 5 mL elementos de esporos; 2,5 mL 20% NH_4NO_3 (p/v); 10 mL 50% glicerol (v/v); 40 mL 1M MES pH 5,5; 10 mL 20% glicose (p/v); 2 mL 100 mM acetoseringona; 1 L dH_2O estéril) suplementado com canamicina (50 mg/mL) que foi mantido sob agitação a 28°C até OD_{600} atingir 0,25 (Figura 11 D).

A suspensão de esporos de *F. virguliforme* (Figura 11 E) foi preparada adicionando 10 mL de dH_2O estéril a placas MA 2% cultivadas em meio SNA + cravo por 3 semanas a 25°C com 12h de fotoperíodo. Após a raspagem das placas, foi feita a filtragem dos esporos em duas camadas de gaze estéril e ajuste da concentração para 1×10^6 conídios/mL. Volumes iguais da cultura bacteriana e suspensão de conídios foram transferidos para microtubos de 2 mL que foram incubados por 20 min em temperatura ambiente. Em seguida, 200 µL da mistura foram transferidos para membranas de nitrocelulose (0,45 µm, ø 90 mm, Sartorius Stedim Biotech, Alemanha) em placa de Petri (ø 100 mm) com meio de co-cultivo (CM; o mesmo que IM com a exceção de que 5 mL de glicose a 20% e 20 g de agar foram adicionados) (Figura 11 F).

Após 3 dias de incubação em temperatura ambiente, a membrana foi transferida para placa de Petri com meio de seleção (SM; 40 g de BDA, 1 L de dH_2O) suplementado com 300 µg/mL de higromicina-b (HYG/B), 100 mg/mL de cefotaxima e 100 mg/mL de moxalactam (Figura 11 G e H). As placas foram incubadas em temperatura ambiente por 1 semana para a seleção de colônias resistentes a HYG-B. Os possíveis transformantes foram transferidos para placas de BDA suplementadas com antibiótico (100 mg/mL de cefotaxima e 100 mg/mL de moxalactam). Culturas monospóricas foram obtidas e lâminas de vidro foram preparadas e avaliadas sob microscópio de fluorescência (Axio Imager.A2, Zeiss, EUA)

4. RESULTADOS

Apesar das diversas tentativas, não foi possível obter um transformante de *F. virguliforme* contendo o gene eGFP.

REFERÊNCIAS

BETTS, M. F. et al. Development of a high throughput transformation system for insertional mutagenesis in Magnaporthe oryzae. **Fungal Genetics and Biology**, v. 44, n. 10, p. 1035–1049, out. 2007.

DONG, Y.-H.; WANG, S.-T. Agrobacterium tumefaciens-Mediated Transformation Method for Fusarium oxysporum. Em: COLEMAN, J. (Ed.). **Fusarium wilt: Methods and Protocols**. New York, NY: Springer US, 2022. p. 63–73.

FRANDSEN, R. J. N. A guide to binary vectors and strategies for targeted genome modification in fungi using *Agrobacterium tumefaciens*-mediated transformation. **Journal of Microbiological Methods**, v. 87, n. 3, p. 247–262, 1 dez. 2011.

IDNURM, A. et al. A silver bullet in a golden age of functional genomics: the impact of Agrobacterium-mediated transformation of fungi. **Fungal Biology and Biotechnology**, v. 4, n. 1, p. 6, 26 set. 2017.

LIU, T. et al. *Agrobacterium*-mediated transformation as a useful tool for the molecular genetic study of the phytopathogen *Curvularia lunata*. **European Journal of Plant Pathology**, v. 126, n. 3, p. 363–371, 1 mar. 2010.

MALZ, S. et al. Identification of a gene cluster responsible for the biosynthesis of aurofusarin in the *Fusarium graminearum* species complex. **Fungal genetics and biology: FG & B**, v. 42, n. 5, p. 420–433, maio 2005.

PUDAKE, R. N. et al. Investigation of the *Fusarium virguliforme* FvTox1 mutants revealed that the FvTox1 toxin is involved in foliar sudden death syndrome development in soybean. **Current Genetics**, v. 59, n. 3, p. 107–117, 1 ago. 2013.

SØRENSEN, L. Q. et al. Genetic transformation of *Fusarium avenaceum* by *Agrobacterium tumefaciens* mediated transformation and the development of a USER-Brick vector construction system. **BMC Molecular Biology**, v. 15, n. 1, p. 15, 22 jul. 2014.

VISENTIN, I. et al. Transcription of Genes in the Biosynthetic Pathway for Fumonisin Mycotoxins Is Epigenetically and Differentially Regulated in the Fungal Maize Pathogen *Fusarium verticillioides*. **Eukaryotic Cell**, v. 11, n. 3, p. 252–259, mar. 2012.

CAPÍTULO 5 - DETECÇÃO DOS GENES FvTox1 E FvNIS1 EM DIFERENTES ESPÉCIES DO COMPLEXO DE ESPÉCIES *Fusarium solani* POR PCR

1. INTRODUÇÃO

A síndrome da morte súbita da soja, cujos agentes causais são diferentes espécies de *Fusarium* do Complexo de Espécies *Fusarium solani* (Aoki *et al*. 2003, 2005, 2012), apresenta dois tipos de sintomas: os radiculares, conhecidos como podridão e necrose dos tecidos e, os foliares caracterizados por clorose e necrose internerval, que são mais facilmente observados após o estádio reprodutivo da soja (Hartman et al. 2015).

Os sintomas foliares são decorrentes da ação de toxinas produzidas pelo patógeno nas raízes que são translocadas para os tecidos foliares e duas destas toxinas são codificadas pelos genes FvTox1 e FvNIS1 identificados em *F. virguliforme* (Brar et al., 2011; Pudake et al., 2013; Chang et al., 2016). Apesar das demais espécies causadoras da síndrome da morte súbita induzirem sintomas foliares similares aos de *F. virguliforme*, não há relatos sobre a presença desses genes também nestas espécies.

2. OBJETIVO

O objetivo deste trabalho foi verificar através de PCR se os genes FvTox1 e FvNIS1 estão presentes no genoma dos demais agentes causais da síndrome da morte súbita da soja.

3. MATERIAL E MÉTODOS

3.1. Desenho de primers

O desenho dos pares de primers Tox1-F + Tox1-R e NIS1-F + NIS1-R (Tabela 3) para amplificar, respectivamente, fragmentos dos genes FvTox1 (JF440964.1) e FvNIS1 (GBJV01011406.1) foi feito utilizando a ferramenta PCR Primer Design – Eurofins Genomics (https://eurofinsgenomics.com/en/resources/tools/pcr-primer-design/).

3.2. Seleção de isolados, extração de DNA, PCR e sequenciamento

Foram selecionados n = 39 isolados (n = 16 Clado 2; n = 23 Clado 3) para esse experimento (Tabela 4). Os isolados foram cultivados em meio MA2% líquido por 3 dias em temperatura ambiente sob agitação (100 rpm). O DNA foi extraído da biomassa fúngica utilizando o Wizard® Genomic DNA purification kit (Promega, EUA) de acordo com as instruções do fabricante. A concentração e qualidade do DNA foi confirmada utilizando NanoDrop One™ (ThermoFisher Scientific, EUA).

A PCR foi realizada utilizando o kit AmpliTaq™ DNA Polymerase with Buffer II (Applied Biosystems, ThermoFisher Scientific, EUA) nas seguintes condições de amplificação: 95°C – 2 min, 40 ciclos 95°C – 15s, 55°C – 30s, 72 °C – 20s, 72°C – 5 min, 4°C – hold. Os

produtos de amplificação esperado dos pares de primers Tox1-F + Tox1-R e NIS1-F + NIS1-R eram, respectivamente, 216 bp e 203 bp. A confirmação do resultado foi feita em gel de agarose 1,5% corado com GelRed® (Biotium, EUA) e visualizado em transiluminador MiniBIS (DNR Bio-Imaging Systems, Israel). O isolado CML 2234 – NRRL 34551 de *F. virguliforme* foi utilizado como controle positivo. Um subset de n = 13 isolados foi selecionado o preparo de um gel final (Figura 12).

Os fragmentos amplificados de um representante de *F. virguliforme* (CML 2234 – NRRL 34551), *F. tucumaniae* (CML 2448) e *F. paranaense* (CML 860) foram purificados e sequenciados nas duas direções pela empresa Psomagen (Rockville, EUA). A ferramenta Nucleotide BLAST® (https://blast.ncbi.nlm.nih.gov/Blast.cgi) foi utilizada para comparar o resultado do sequenciamento com sequências do banco de dados do GenBank.

4. RESULTADOS

Um fragmento de aproximadamente 250 bp foi amplificado nas PCRs dos genes FvTox1 e FvNIS1 em todos os isolados membros do Clado 2 do FSSC. Dentre os isolados do Clado 3 do FSSC, foi obtido três resultados negativos na PCR de amplificação do fragmento do gene FvTox1 e um negativo para o fragmento do gene FvNIS1 (Tabela 4).

Com a ferramenta Nucleotide BLAST® identificamos uma sobreposição de 99% e identidade de 100% do resultado do sequenciamento do fragmento gene FvTox1 com a sequência original (JF440964.1). Para o gene FvNIS1, verificamos uma sobreposição de 78% e identidade de 100% do resultado do sequenciamento com a sequência original (GBJV01011406.1).

5. DISCUSSÃO

Com este trabalho preliminar evidenciamos que as demais espécies do Clado 2 do FSSC, *F. tucumaniae*, *F. brasiliense* e *F. crassistipitatum*, que são patogênicas à soja também possuem em seu genoma os genes FvTox1 e FvNIS1 até então identificados em apenas *F. virguliforme*. Fato ainda mais curioso, é a presença destes mesmos genes também no genoma de membros do Clado 3 do FSSC como *F. paranaense*, uma espécie previamente relatada como incapaz de induzir sintomas foliares em soja (Costa et al., 2016) e, *F. solani* FSSC 5, uma espécie que se acredita ser um patógeno facultativo de diversas culturas agrícolas (Chitrampalam e Nelson 2016)

Sabemos que esses genes codificam toxinas diretamente relacionadas com o desenvolvimento da clorose e necrose do tecido foliar (Brar et al. 2011; Pudake et al. 2013; Chang et al. 2016) característica da síndrome da morte súbita da soja, porém, com este trabalho

conseguimos apenas confirmar a presença dos mesmos no genoma das espécies avaliadas. Com a condução de estudos complementares será possível verificar a expressão gênica durante a interação planta-patógeno e avaliar o motivo pelo qual diferentes isolados de uma mesma espécie podem ou não conter estes genes em seu genoma. Em adição, devido a falta de informação sobre a interação *F. paranaense*-soja e também pelo evidenciado neste trabalho, novos estudos são necessários para elucidar o desenvolvimento da sintomatologia durante o processo desta interação.

REFERÊNCIAS

AOKI, T. et al. Sudden-death syndrome of soybean is caused by two morphologically and phylogenetically distinct species within the *Fusarium solani* species complex — *F. virguliforme* in North America and *F. tucumaniae* in South America. **Mycologia**, v. 95, n. 4, p. 660–684, jul. 2003.

AOKI, T.; O'DONNELL, K.; SCANDIANI, M. M. Sudden death syndrome of soybean in South America is caused by four species of *Fusarium*: *Fusarium brasiliense* sp. nov., *F. cuneirostrum* sp. nov., *F. tucumaniae*, and *F. virguliforme*. **Mycoscience**, v. 46, n. 3, p. 162–183, 1 jun. 2005.

AOKI, T.; SCANDIANI, M. M.; O'DONNELL, K. Phenotypic, molecular phylogenetic, and pathogenetic characterization of *Fusarium crassistipitatum* sp. nov., a novel soybean sudden death syndrome pathogen from Argentina and Brazil. **Mycoscience**, v. 53, n. 3, p. 167–186, 1 maio 2012.

BRAR, H. K.; SWAMINATHAN, S.; BHATTACHARYYA, M. K. The *Fusarium virguliforme* Toxin FvTox1 Causes Foliar Sudden Death Syndrome-Like Symptoms in Soybean. **Molecular Plant-Microbe Interactions®**, v. 24, n. 10, p. 1179–1188, out. 2011.

CHANG, H.-X. et al. Identification of Multiple Phytotoxins Produced by *Fusarium virguliforme* Including a Phytotoxic Effector (FvNIS1) Associated With Sudden Death Syndrome Foliar Symptoms. **Molecular Plant-Microbe Interactions®**, v. 29, n. 2, p. 96–108, fev. 2016.

CHITRAMPALAM, P.; NELSON, B. 2016. Multilocus phylogeny reveals an association of agriculturally important *Fusarium solani* species complex (FSSC) 11, and clinically important FSSC 5 and FSSC 3 + 4 with soybean roots in the north central United States. **Antonie van Leeuwenhoek**, v. 109, n. 2, fev. 2016.

COSTA, S. S. et al. *Fusarium paranaense* sp. nov., a member of the *Fusarium solani* species complex causes root rot on soybean in Brazil. **Fungal Biology**, v. 120, n. 1, p. 51–60, jan. 2016.

HARTMAN, G. L.; CHANG, H.-X.; LEANDRO, L. F. Research advances and management of soybean sudden death syndrome. **Crop Protection**, Ecology and management of *Fusarium* diseases. v. 73, p. 60–66, 1 jul. 2015.

PUDAKE, R. N. et al. Investigation of the *Fusarium virguliforme* FvTox1 mutants revealed that the FvTox1 toxin is involved in foliar sudden death syndrome development in soybean. **Current Genetics**, v. 59, n. 3, p. 107–117, 1 ago. 2013.

Table 1. Strains of *Fusarium solani* used in this study

				GenBank Accession no.	
CML[1]	**Species**	**Geographic origin[2]**	**Year**	**RPB2**	**L44**
FSSC Clade 3					
4453	*F. paranaense*	Ponta Porã, MS	2020		
4456 *	*F. paranaense*	Primavera do Leste, MT	2021		
4457	*F. paranaense*	Chapadão do Sul, MS	2021		
4467	*F. paranaense*	Lucas do Rio Verde, MT	2019		
4468	*F. paranaense*	Lucas do Rio Verde, MT	2019		
4469	*F. paranaense*	Lucas do Rio Verde, MT	2020		
4475	*F. paranaense*	Chapadão do Sul, MS	2020		
4477	*F. paranaense*	Santo Antônio de Goiás, GO	2021		
4479	*F. paranaense*	Nova Marilândia, MT	2021		
4481	*F. paranaense*	Nova Marilândia, MT	2021		
4483	*F. paranaense*	Primavera do Leste, MT	2021		
4484	*F. paranaense*	São Gabriel do Oeste, MS	2021		
4485	*F. paranaense*	São Gabriel do Oeste, MS	2021		
4491	*F. paranaense*	Cruz Alta, RS	2022		
4492	*F. paranaense*	Aral Moreira, MS	2022		
4493	*F. paranaense*	Aral Moreira, MS	2022		
4452	*F. solani*	Madre de Deus de Minas, MG	2019		
4458 *	*F. solani*	Rio Verde, GO	2021		
4463	*F. solani*	Arambaré, RS	2021		
4478	*F. solani*	Diamantino, MT	2021		
4480	*F. solani*	Rio Verde, GO	2021		
4482	*F. solani*	Diamantino, MT	2021		
4486	*F. solani*	Santo Antônio de Goiás, GO	2021		
4487	*F. solani*	Chapadão do Céu, GO	2022		
4488	*F. solani*	Ernestina, RS	2022		
4489	*F. solani*	Ernestina, RS	2022		
4490	*F. solani*	Cruz Alta, RS	2022		
FSSC Clade 2					
4465	*F. brasiliense*	Madre de Deus de Minas, MG	2019		
4466 *	*F. brasiliense*	Madre de Deus de Minas, MG	2019		
4460	*F. crassistipitatum*	Luminárias, MG	2020		
4461 *	*F. crassistipitatum*	Ipameri, GO	2020		
4476	*F. crassistipitatum*	Luminárias, MG	2020		
4454	*F. tucumaniae*	Madre de Deus de Minas, MG	2019		
4455	*F. tucumaniae*	Madre de Deus de Minas, MG	2019		
4459 *	*F. tucumaniae*	Madre de Deus de Minas, MG	2019		
4470	*F. tucumaniae*	Luminárias, MG	2020		

[1] CML = Coleção Micológica de Lavras, Departamento de Fitopatologia, Universidade Federal de Lavras, Lavras, Minas Gerais, Brazil
[2] Brazilian states: MG = Minas Gerais; MT = Mato Grosso; MS = Mato Grosso do Sul; GO = Goiás; RS = Rio Grande do Sul
* Indicates isolates selected for the pathogenicity test

Table 2. Disease severity and root necrosis of soybean (*Glycine max* L.) plants 35 days after the inoculation with different *Fusarium solani* species

Code	Species	Disease severity	Root necrosis
CML 4456	*F. paranaense*	2.75 ± 1.29[1] **	1.67 ± 0.64 [a]
CML 4458	*F. solani*	2.92 ± 1.51 **	1.12 ± 0.46 [a]
CML 4459	*F. tucumaniae*	2.58 ± 1.24 *	1.48 ± 0.73 [a]
CML 4461	*F. crassistipitatum*	3.50 ± 1.00 ***	1.49 ± 0.47 [a]
CML 4466	*F. brasiliense*	2.83 ± 1.11 **	1.23 ± 0.84 [a]
Control		1.00 ± 0.00	0.00 ± 0.00 [b]

[1] Mean ± standard deviation

Asterisks indicates significant difference according to Dunn's test between each treatment when compared to the control; * = $p \leq 0.05$; ** = $p \leq 0.01$; *** = $p \leq 0.001$

Lower case letters indicate significant difference ($p \leq 0.05$) according to Scott-Knott's test

Tabela 3. Lista de primers

Nome	**Sequência (5’ – 3’)**
gRNA_F	CCGGAATTCACTGATGATTACG
gRNA_R	CGCGGATCCTCTCTAGAGT
P1.Tox1_F	AACCTACAACACCCATCGCTAACGG
P2.Tox1_R	AAAACCCGTTAGCGATGGGTGTTGT
P1.NIS1_F	AACCTAGGACCGAGATAGAACGAGT
P2.NIS1_R	AAAACACTCGTTCTATCTCGGTCCT
M13F	CGCCAGGGTTTTCCCAGTCACGAC
M13R	CAGGAAACAGCTATGAC
HYG/F	CTCTAGTTCTAGACTCTAGTGGATCCACAGAAGATGATATTGAAGGAGC
HYG/R	CTCTAGTGAATTCGTCGACTTAATAACACATTGCGGACGT
Tox1-F	AGAGAACAGGCACGCTGGAATG
Tox1-R	TGGCACCAGCCTCGACAAATAC
NIS1-F	AGTCGCCGACTCGTTCTATCTC
NIS1-R	ACTCCTTGCTGGTCTTGTCTCC

Tabela 4. Isolados de *Fusarium solani* cujos fragmentos dos genes FvTox1 e FvNIS1 foram amplificados por PCR

			Resultado PCR	
CML	**Espécie**	**Origem**	**TOX1**	**NIS1**
Clado 3 FSSC				
860 *	*F. paranaense*	Brasília, DF	+	+
1830	*F. paranaense*	Cristalina, GO	+	+
2043	*F. solani*	Sebastião Laranjeiras, BA	+	+
4452	*F. solani*	Madre de Deus de Minas, MG	+	+
4453	*F. paranaense*	Ponta Porã, MS	+	+
4456	*F. paranaense*	Primavera do Leste, MT	+	+
4457	*F. paranaense*	Chapadão do Sul, MS	+	+
4458	*F. solani*	Rio Verde, GO	+	+
4463	*F. solani*	Arambaré, RS	+	+
4467	*F. paranaense*	Lucas do Rio Verde, MT	+	+
4468	*F. paranaense*	Lucas do Rio Verde, MT	+	+
4469	*F. paranaense*	Lucas do Rio Verde, MT	+	+
4475	*F. paranaense*	Chapadão do Sul, MS	-	-
4477	*F. paranaense*	Santo Antônio de Goiás, GO	+	+
4478	*F. solani*	Diamantino, MT	+	+
4479	*F. paranaense*	Nova Marilândia, MT	+	+
4480	*F. solani*	Rio Verde, GO	-	+
4481	*F. paranaense*	Nova Marilândia, MT	+	+
4482	*F. solani*	Diamantino, MT	+	+
4483	*F. paranaense*	Primavera do Leste, MT	-	+
4484	*F. paranaense*	São Gabriel do Oeste, MS	+	+
4485	*F. paranaense*	São Gabriel do Oeste, MS	+	+
4487	*F. solani*	Chapadão do Céu, GO	+	+
Clado 2 FSSC				
1882	*F. crassistipitatum*	Cristalina, GO	+	+
1886	*F. brasiliense*	Califórnia, EUA	+	+
1887	*F. phaseoli*	Michigan, EUA	+	+
1890	*F. tucumaniae*	Brasília, DF	+	+
2044	*F. virguliforme*	Kansas, EUA	+	+
2229	*F. cuneirostrum*	EUA	+	+
2231	*F. brasiliense*	Brasília, DF	+	+
2234 *	*F. virguliforme*	San Pedro, Buenos Aires, Argentina	+	+
2448 *	*F. tucumaniae*	Guarapuava, PR	+	+
4454	*F. tucumaniae*	Madre de Deus de Minas, MG	+	+
4455	*F. tucumaniae*	Madre de Deus de Minas, MG	+	+
4459	*F. tucumaniae*	Madre de Deus de Minas, MG	+	+
4460	*F. crassistipitatum*	Luminárias, MG	+	+
4461	*F. crassistipitatum*	Ipameri, GO	+	+
4462	*Fusarium* sp.	Arambaré, RS	+	+
4465	*F. brasiliense*	Madre de Deus de Minas, MG	+	+
4466	*F. brasiliense*	Madre de Deus de Minas, MG	+	+
4470	*F. tucumaniae*	Luminárias, MG	+	+
4476	*F. crassistipitatum*	Luminárias, MG	+	+

[1] CML = Coleção Micológica de Lavras, Departamento de Fitopatologia, Universidade Federal de Lavras, Lavras, Minas Gerais, Brasil
[2] Estados brasileiros: MG = Minas Gerais; MT = Mato Grosso; MS = Mato Grosso do Sul; GO = Goiás; RS = Rio Grande do Sul
* Indica isolados selecionados para o sequenciamento dos genes FvTox1 FvNIS1

Table S1. FSSC reference strains used in the phylogeny analysis

Code[1]	Species	Substrate	Origin[2]	GenBank accession number	
				RPB2	L44
CML 1830^{HT}	*F. paranaense*	*Glycine max*	Cristalina, GO	KF680011	
CML 860^{PT}	*F. paranaense*	*Glycine max*	Brasília, DF	KF680005	
CML 1993	*F. paranaense*	*Glycine max*	Marinalva, PR	KF680004	
CBS 475.67^{T}	*F. falciforme*	Human	Puerto Rico	LT960558	
CML 3972	*F. suttonianum*	*Citrullus lanatus*	Cantá, RR	MK988365	
NRRL 32858^{T}	*F. suttonianum*	Human	USA	EU329630	
FRC S-2477^{T}	*F. keratoplasticum*	Plumbing	USA	JN235897	
CBS 115659^{ET}	*F. martii*	*Solanum tuberosum*	Germany	JX435256	
CBS 115658^{T}	*F. noneumartii*	*Solanum tuberosum*	Israel	LR583852	
CBS 140079^{ET}	*F. solani*	*Solanum tuberosum*	Slovenia	KT313623	
NRRL 25388	*F. solani*	Human	India	MH582411	
NRRL 54969	*F. solani*			KC808333	
NRRL 22570^{T}	*F. piperis*	*Piper nigrum*	Brazil	EU329513	
NRRL 20101	*F. striatum*	Cotton clothes	Panama	EU329490	
NRRL 54364^{T}	*F. azukicola*	*Vigna angularis*	Japan	KJ511287	
NRRL 22825	*F. virguliforme*	*Glycine max*	USA	EU329533	JF920191
NRRL 31041^{T}	*F. virguliforme*	*Glycine max*	USA	JX171643	JF920192
NRRL 36605	*F. virguliforme*	*Glycine max*	Argentina		JF920207
NRRL 36896	*F. virguliforme*	*Glycine max*	Argentina		JF920209
NRRL 32392	*F. virguliforme*	*Glycine max*	USA		JF920202
NRRL 34436	*F. virguliforme*	*Glycine max*	USA		JF920203
NRRL 34551	*F. virguliforme*	*Glycine max*	Argentina		JQ670188
CML 2448	*F. tucumaniae*	*Glycine max*	Guarapuava, PR		
NRRL 31096^{T}	*F. tucumaniae*	*Glycine max*	Argentina	GU170600	JF920193
NRRL 34546	*F. tucumaniae*	*Glycine max*	Argentina	KJ511284	
NRRL 31950	*F. tucumaniae*	*Glycine max*	Ponta Grossa, PR		JQ670185
NRRL 31776	*F. tucumaniae*	*Glycine max*	Tapera, RS		JF920199
NRRL 22411	*F. phaseoli*	*Phaseolus vulgaris*	USA	KJ511278	KF706639
NRRL 22276	*F. phaseoli*	*Phaseolus vulgaris*	USA	JX171608	JF920189
NRRL 31156	*F. phaseoli*	*Phaseolus vulgaris*	USA	KJ511281	JF920195
NRRL 31157^{T}	*F. cuneirostrum*	*Phaseolus vulgaris*	USA	KJ511282	JF920196
NRRL 36023	*F. cuneirostrum*	*Vigna radiata*	Canada		JF920206
NRRL 22275	*F. cuneirostrum*	*Phaseolus vulgaris*	Japan		JF920188
NRRL 31104	*F. cuneirostrum*	*Phaseolus vulgaris*	Japan	EU329558	JF920194
NRRL 31949	*F. crassistipitatum*	*Glycine max*	Cristalina, GO	EU329566	JF920201
NRRL 43825	*F. crassistipitatum*	*Glycine max*	Argentina		JF920280
NRRL 46170	*F. crassistipitatum*	*Glycine max*	Argentina	KJ511286	JF920281
NRRL 46171	*F. crassistipitatum*	*Glycine max*	Argentina		JF920282
NRRL 46173	*F. crassistipitatum*	*Glycine max*	Argentina		JF920283
NRRL 36877^{T}	*F. crassistipitatum*	*Glycine max*	Argentina	FJ240405	JF920208
NRRL 43824	*F. crassistipitatum*	*Glycine max*	Argentina		JF920279
NRRL 46175	*F. crassistipitatum*	*Glycine max*	Argentina		JF920284
NRRL 31757^{T}	*F. brasiliense*	*Glycine max*	Brasília, DF	EU329565	JF920197
NRRL 22743	*F. brasiliense*	*Glycine max*	Brasília, DF	EU329525	
NRRL 31762	*F. brasiliense*	*Glycine max*	Campo Mourão, PR		JF920198
NRRL 31779	*F. brasiliense*	*Glycine max*	Nonoai, RS	KJ511283	KF706641
NRRL 22678	*F. brasiliense*	*Glycine max*	USA		JF920190
NRRL 31756	*F. brasiliense*	*Glycine max*	Brasília, DF		KF706640
NRRL 34938	*F. brasiliense*	*Glycine max*	Passo Fundo, RS		JF920205
NRRL 22090	*F. illudens*	*Beilschmiedia tawa*	New Zealand	JX171601	
NRRL 22632	*F. plagianthi*	*Hoheria glabrata*	New Zealand	JX171614	
NRRL 22153	*F. cucurbiticola* MP-I	*Cucurbita* sp.	USA	EU329492	
NRRL 22400	*F. bataticola* MP-II	*Ipomea batatas*	USA	EU329509	
NRRL 22157	*F. mori* MP-III	*Morus alba*	Japan	EU329493	
NRRL 22163	*F. yamamotoi* MP-IV	*Xanthoxylum piperitum*	Japan	EU329496	
NRRL 28546	*F. petroliphilum* MP-V	Human eye	USA	EU329544	
NRRL 22278	*F. vanettenii* MP-VI	*Pisum sativum*	USA	EU329501	
NRRL 22161	*F. silvicola* MP-VII	*Robinia pseudoacacia*	Japan	EU329494	

[1] CML = Coleção Micológica de Lavras, Departamento de Fitopatologia, Universidade Federal de Lavras, Lavras, Minas Gerais, Brazil; CBS = Westerdijk Fungal Biodiversity Institute, Utrecht, The Netherlands; NRRL = Northern Regional Research Laboratory, Peoria, Illinois, USA; FRC = Fusarium Research Center, Pennsylvania State University, Pennsylvania, USA; HT = holotype; PT = paratype; T = type; ET = epitype.

[2] Brazilian states; GO = Goiás, PR = Paraná; DF = Distrito Federal; RR = Roraima; RS = Rio Grande do Sul

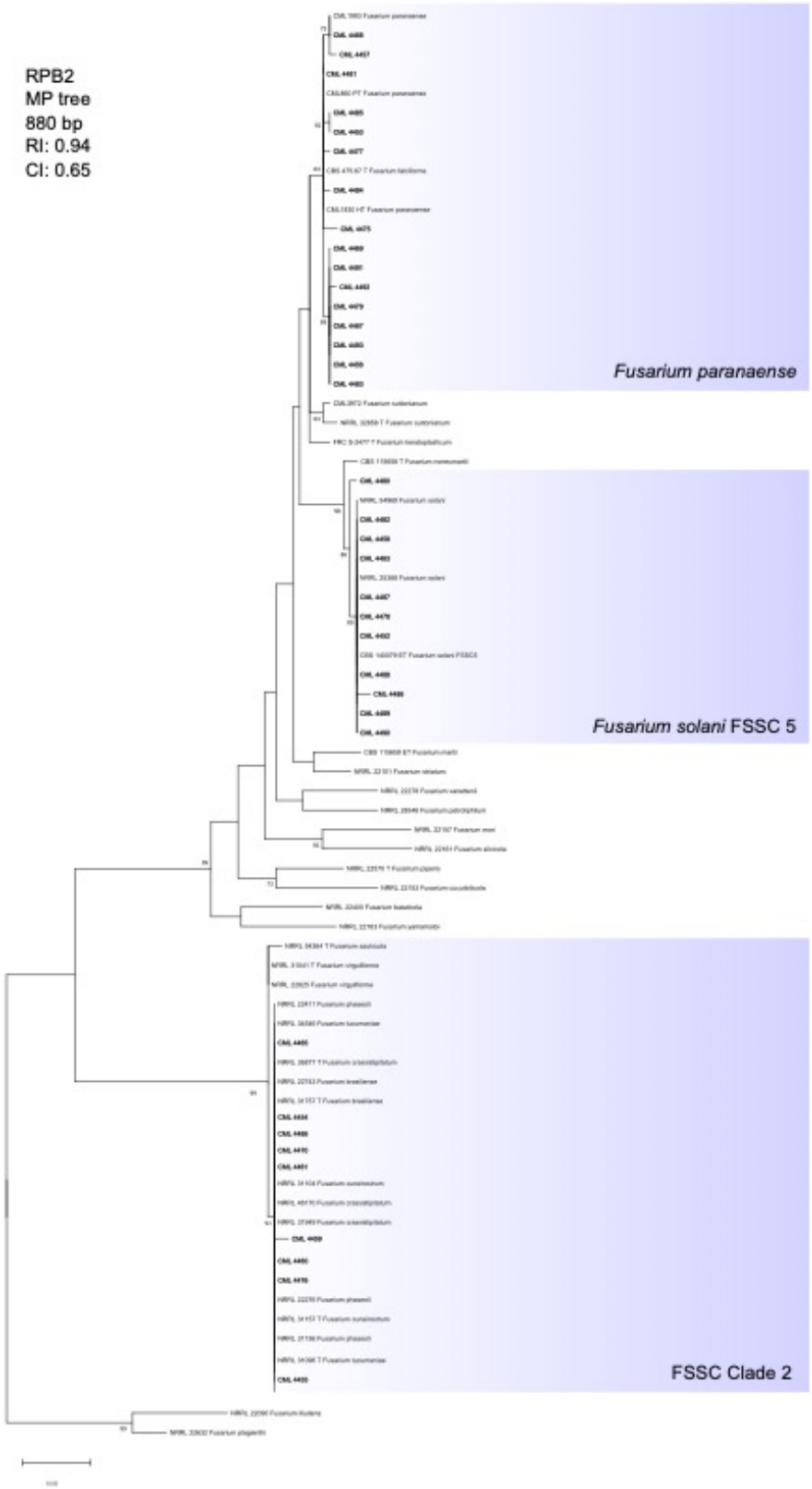

Figure 1. Maximum parsimony phylogenetic tree inferred from partial RPB2 sequences showing the relatedness of *Fusarium* species associated with soybean (*Glycine max* L.) with other species from the *Fusarium solani* species complex. Bootstrap values ≥ 70% are shown at the internodes. Ex-type strains are indicated with T, ex- epitype strains with ET, ex-holotype strain with HT and ex-paratype strain with PT. *Fusarium illudens* (NRRL 22090) and *Fusarium plagianthi* (NRRL 22632) were used as outgroup.

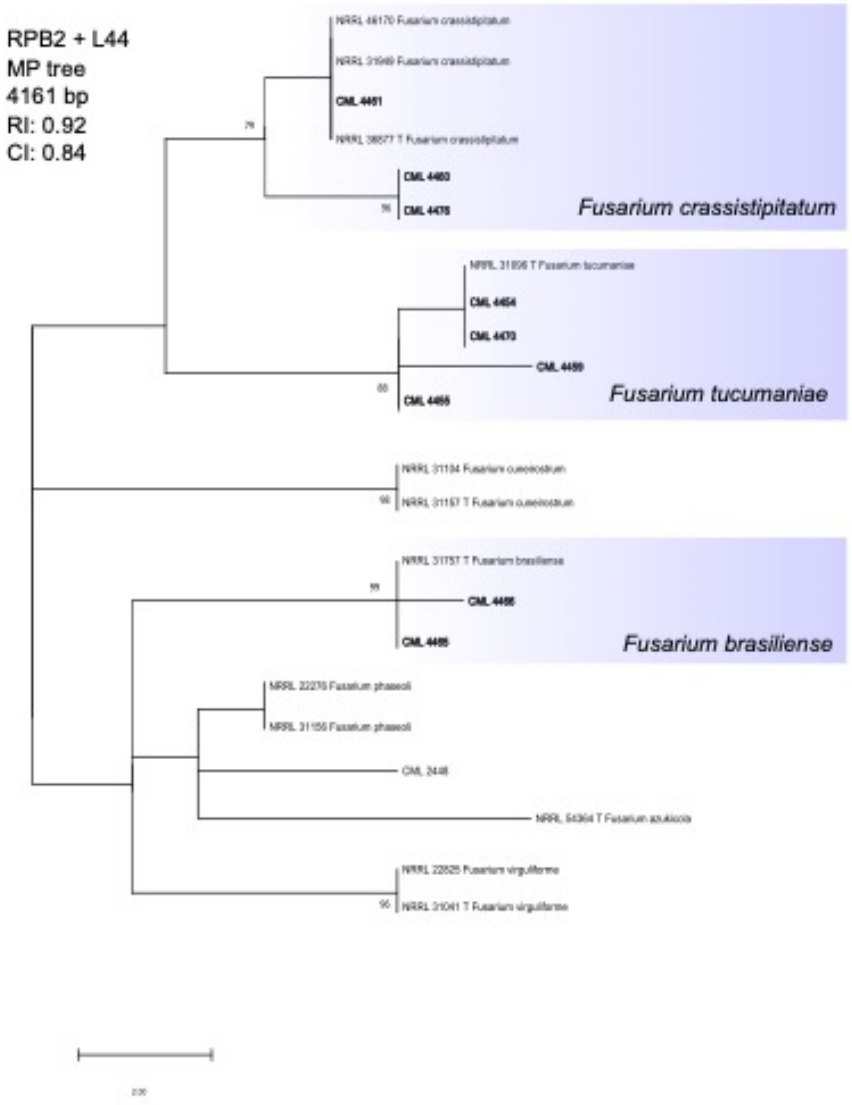

Figure 2. Maximum parsimony phylogenetic tree inferred from partial RPB2 and L44 sequences showing the relatedness of *Fusarium* species associated with soybean (*Glycine max* L.) with other clade 2 species from the *Fusarium solani* species complex. Bootstrap values ≥ 70% are shown at the internodes. Ex-type strains are indicated with T.

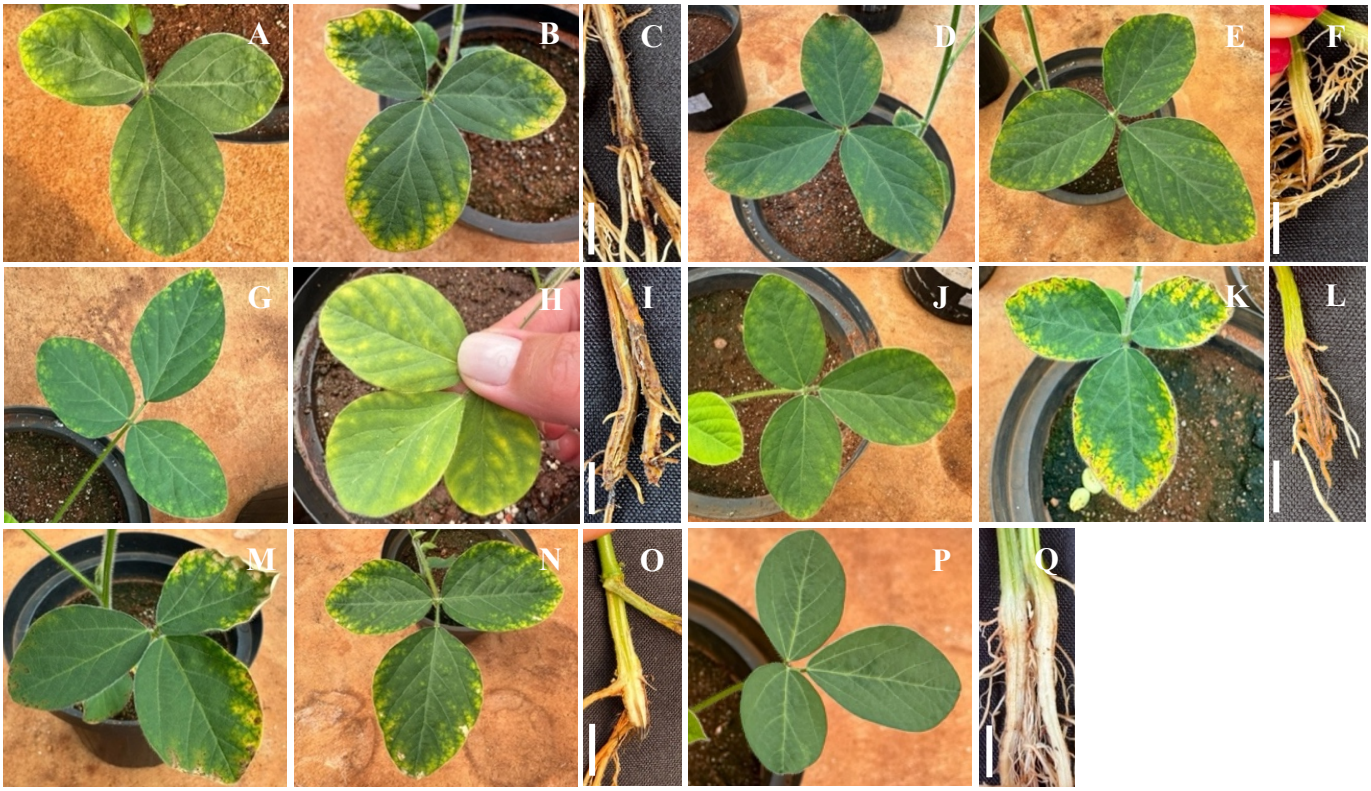

Figure 3. Foliar symptoms and root necrosis of soybean (*Glycine max* L.) plants 35 days after inoculation with different *Fusarium solani* species. **A-C**, *F. paranaense*. **D-F**, *F. solani* FSSC 5. **G-I**, *F. tucumaniae*. **J-L**, *F. brasiliense*. **M-O**, *F. crassistipitatum*. **P-Q**, control. Bars = 1 cm.

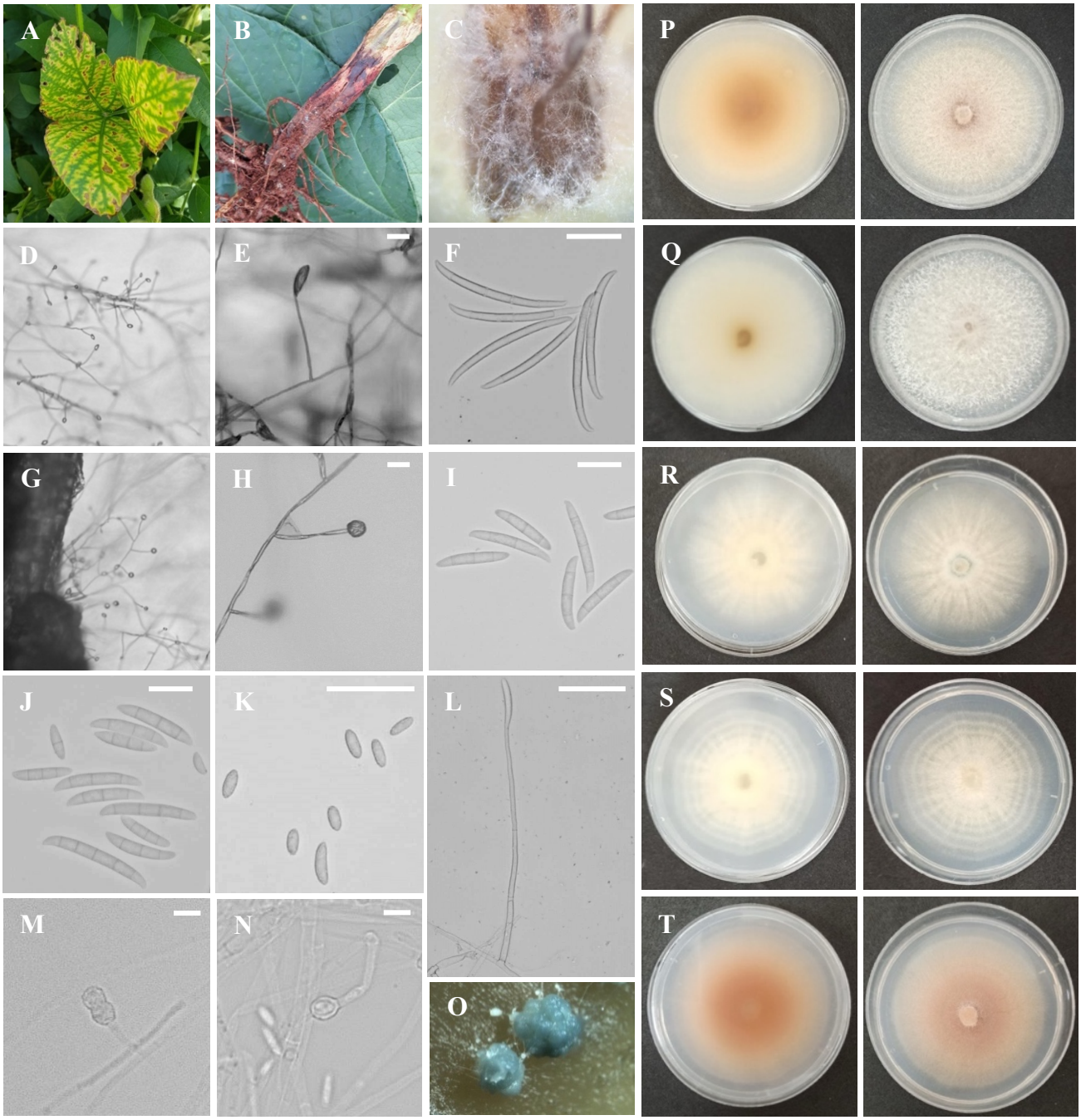

Figure 4. Typical sudden death syndrome of soybean (*Glycine max* L.) symptoms and morphological characteristics of *Fusarium solani* species. **A**, foliar interveinal chlorosis and necrosis. **B**, root tissue necrosis and browning. **C**, FSSC typical sporulation on root fragment. **D-E** Clade 2 monophialides with conidia production in false heads. **F**, Clade 2 sporodochia macroconidia. **G-H**, Clade 3 monophialides with conidia production in false heads. **I**, Clade 3 sporodochia macroconidia. **J-K**, Clade 3 macro and microconidia produced in aerial mycelia. **L**, FSSC typical monophialide. **M-N**, terminal and intercalated chlamydospores. **O**, Clade 2 sporodochia produced in 2% MA plates. **P**, *F. solani* FSSC 5 colony grown on PDA. **Q**, *F. paranaense* colony grown on PDA. **R**, *F. tucumaniae* colony grown on PDA. **S**, *F. crassistipitatum* colony grown on PDA. **T**, *F. brasiliense* colony grown on PDA. Bars: **E, F, H, I-L** = 20 µm. **M-N** = 10 µm.

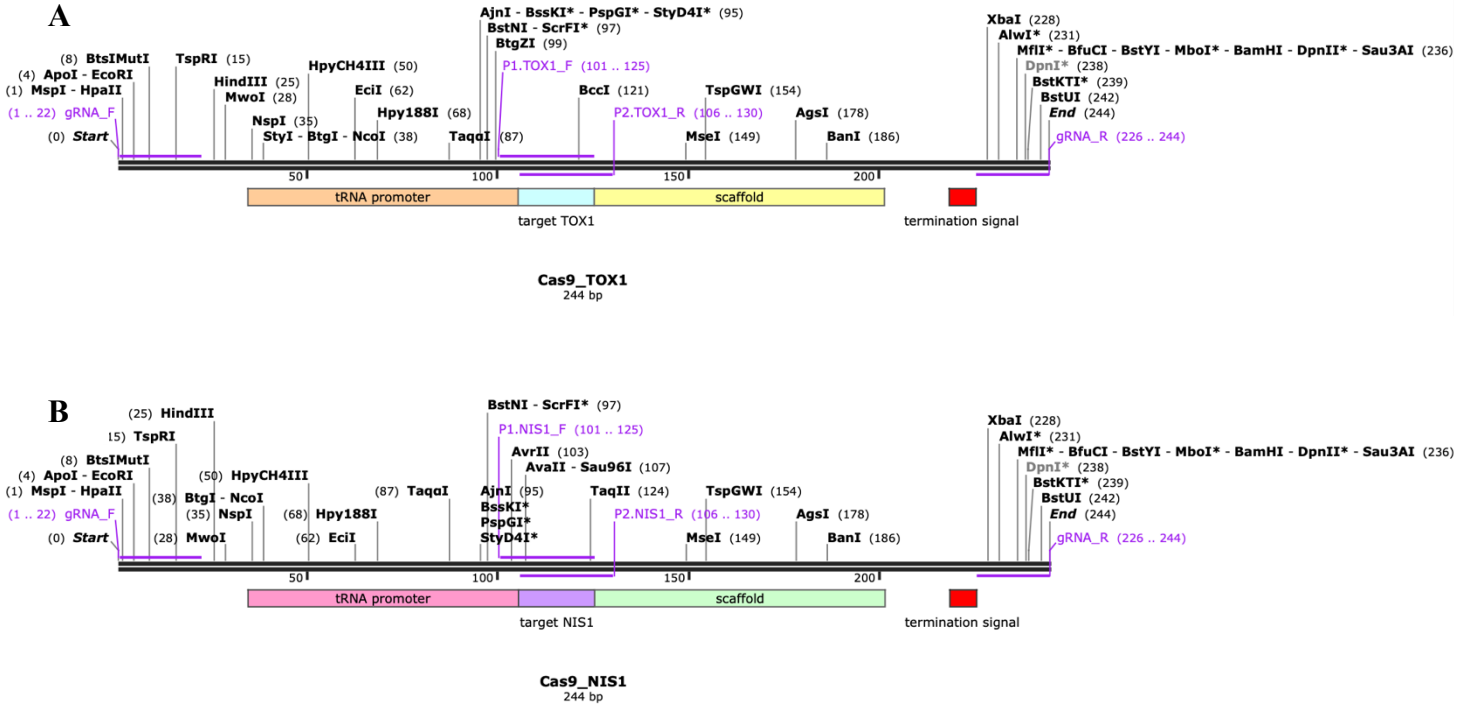

Figura 5. Mapa das cassete criadas neste trabalho. **A.** Tox1. **B.** NIS1.

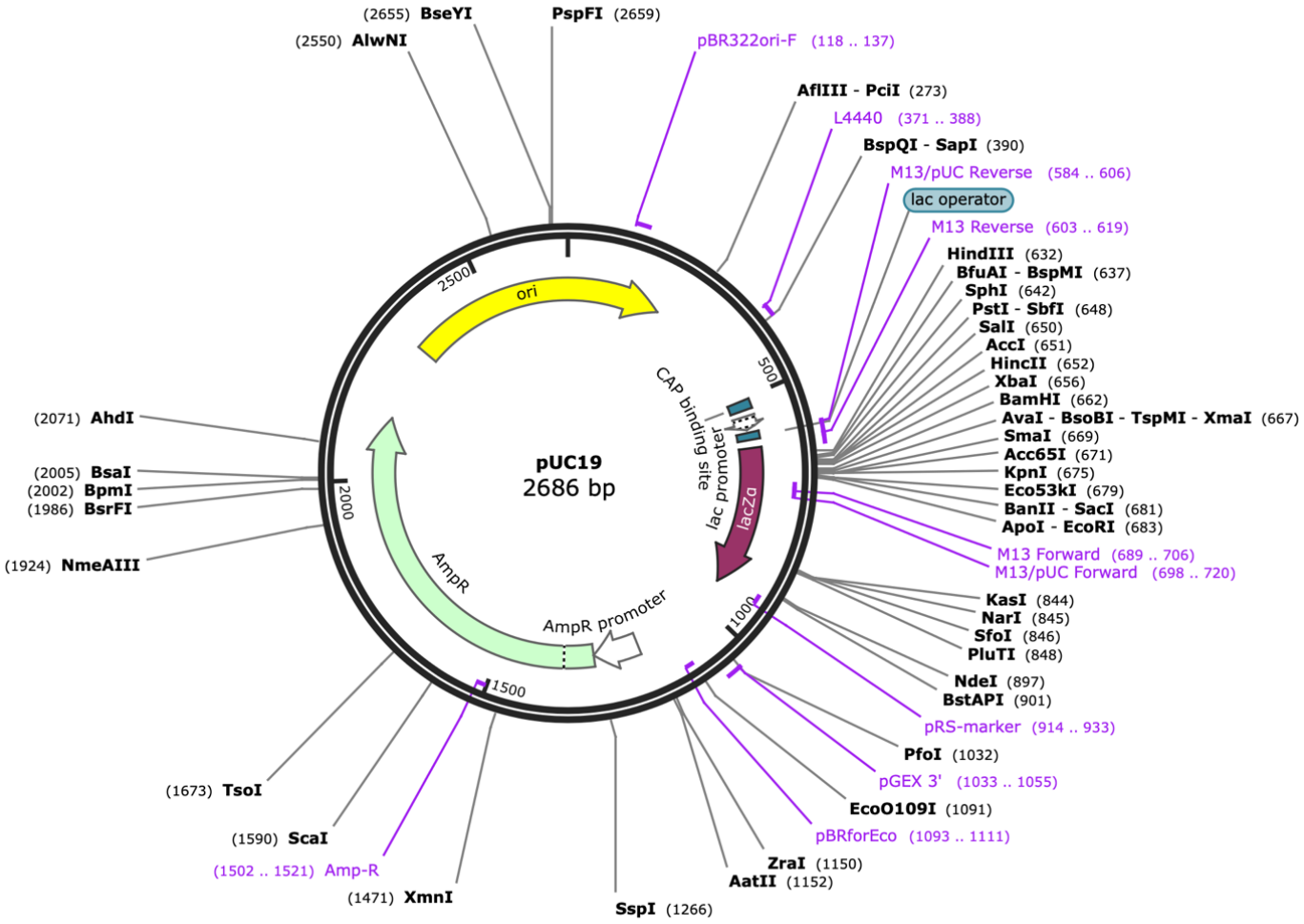

Figura 6. Mapa do vetor pUC19 utilizado neste trabalho.

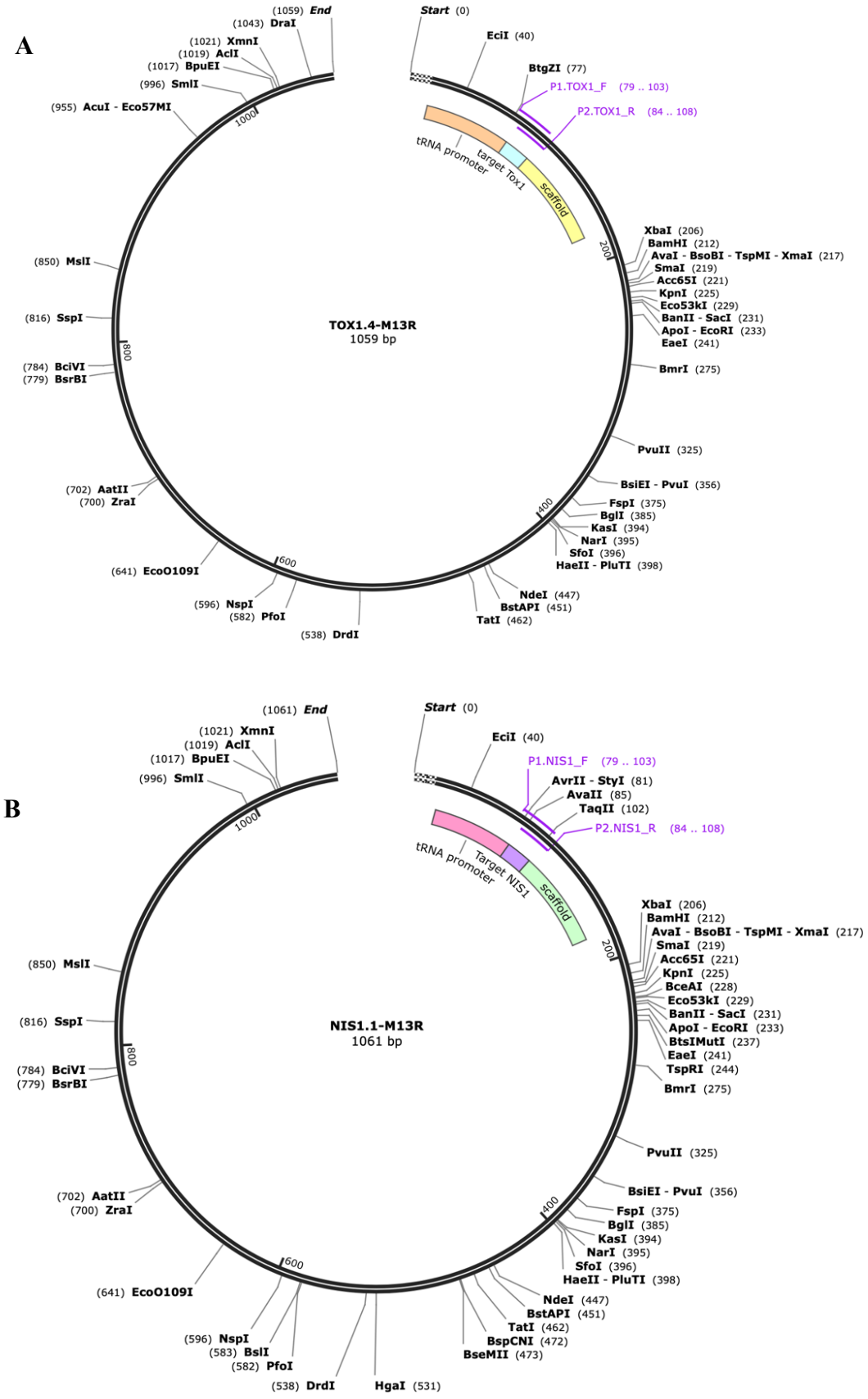

Figura 7. Mapa dos vetores individuais criados neste trabalho. **A.** Tox1#4. **B.** NIS1#1

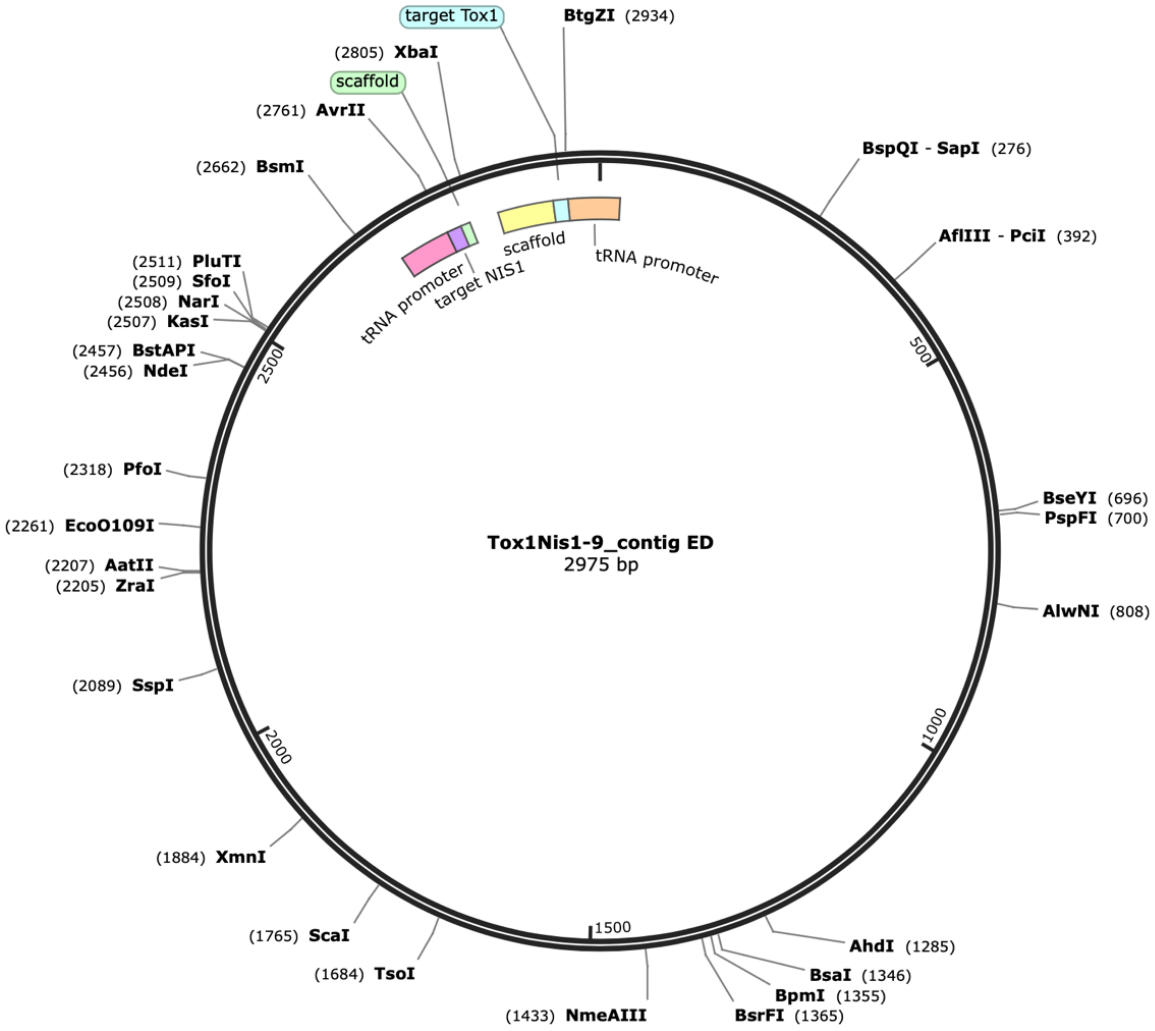

Figura 8. Mapa do vetor Tox1+NIS1#9 criado neste trabalho.

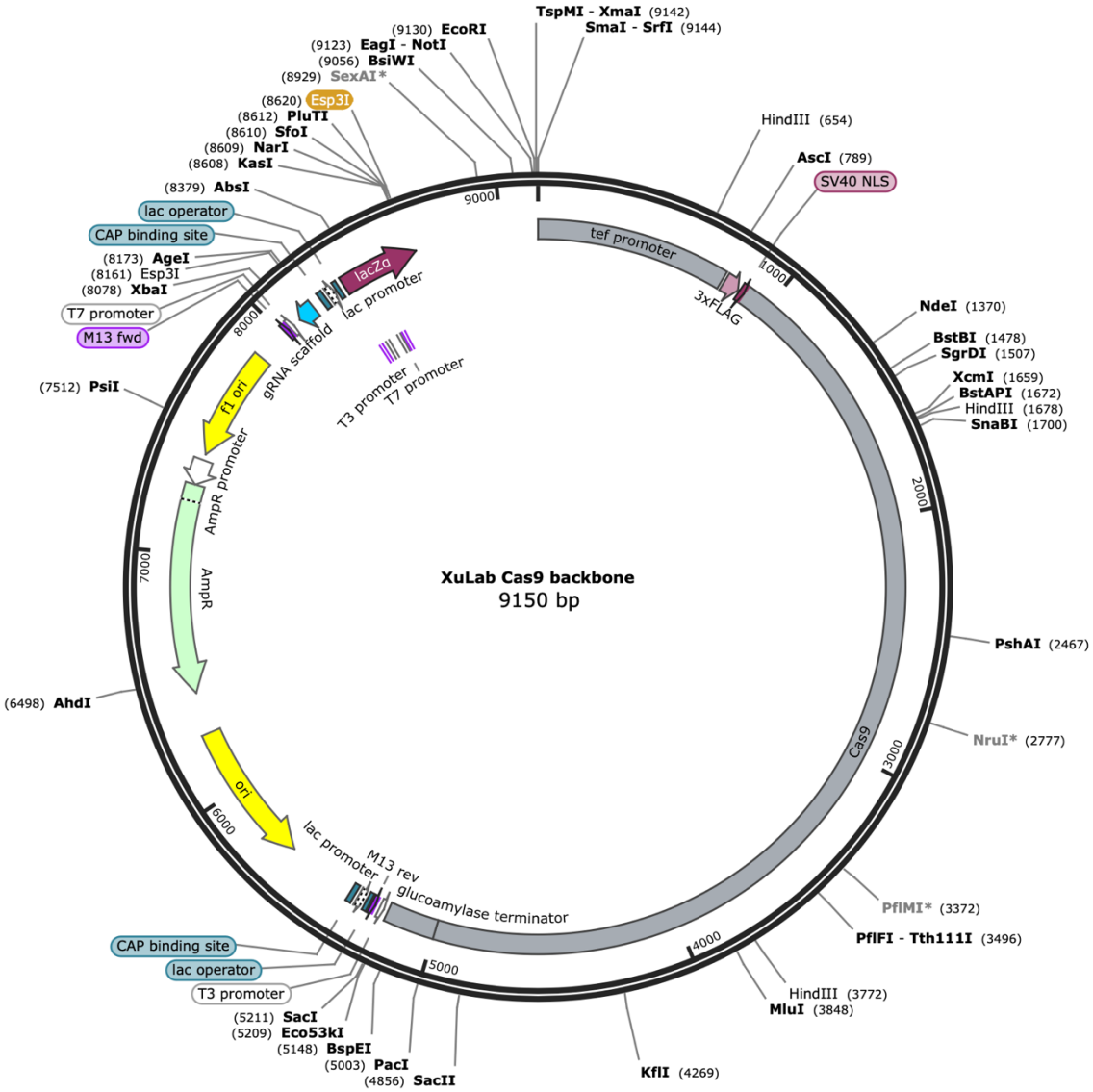

Figura 9. Mapa do vetor contendo o gene Cas9 utilizado neste trabalho.

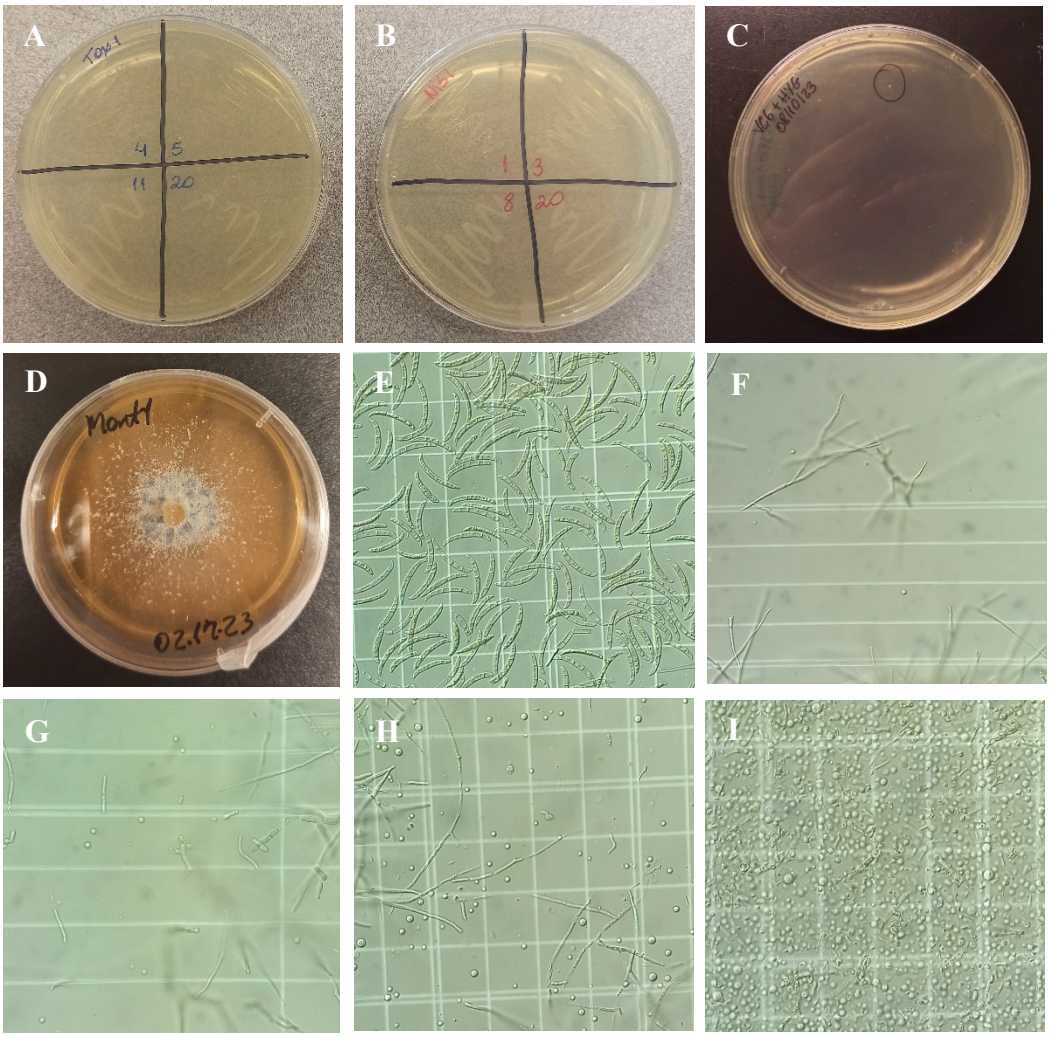

Figura 10. Vetores criados e etapas da obtenção de protoplastos utilizados na edição genética de *Fusarium virguliforme* via CRISPR-Cas9. **A.** *E. coli* após a transformação com vetor Tox1. **B.** *E. coli* após a transformação com vetor NIS1. **C.** *E. coli* após a transformação com vetor hyg-b. **D.** Isolado NRRL 34551 de *F. virguliforme*. **E.** Macroconídios de *F. virguliforme* utilizados para a obtenção de micélio para protoplastização. **F.** Protoplastos de *F. virguliforme* após 1h de incubação. **G.** Protoplastos de *F. virguliforme* após 2h de incubação. **H.** Protoplastos de *F. virguliforme* após 3h de incubação. **I.** Protoplastos de *F. virguliforme* concentrados utilizados na transformação.

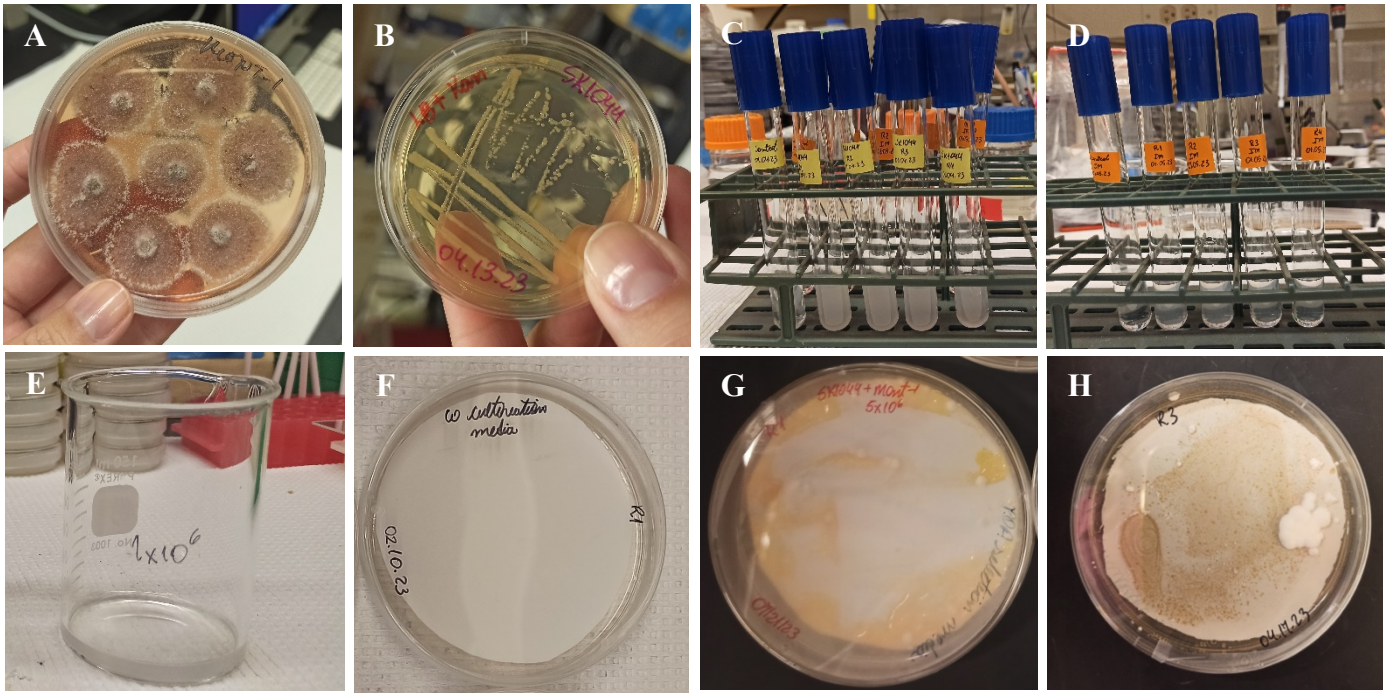

Figura 11. Material biológico utilizado e etapas da transformação de *Fusarium virguliforme* por ATMT. **A.** Isolado NRRL 34551 de *F. virguliforme*. **B.** Cepa SK1044 de *Agrobacterium tumefaciens*. **C.** Cultivo da cepa SK1044 em meio mínimo. **D.** Cultivo da cepa SK1044 em meio de indução. **E.** Suspensão de esporos do isolado NRRL 34551. **F.** Co-cultivo de NRRL 34551 e SK1044. **G e H.** Seleção de colônias resistentes à HYG-B em meio de seleção.

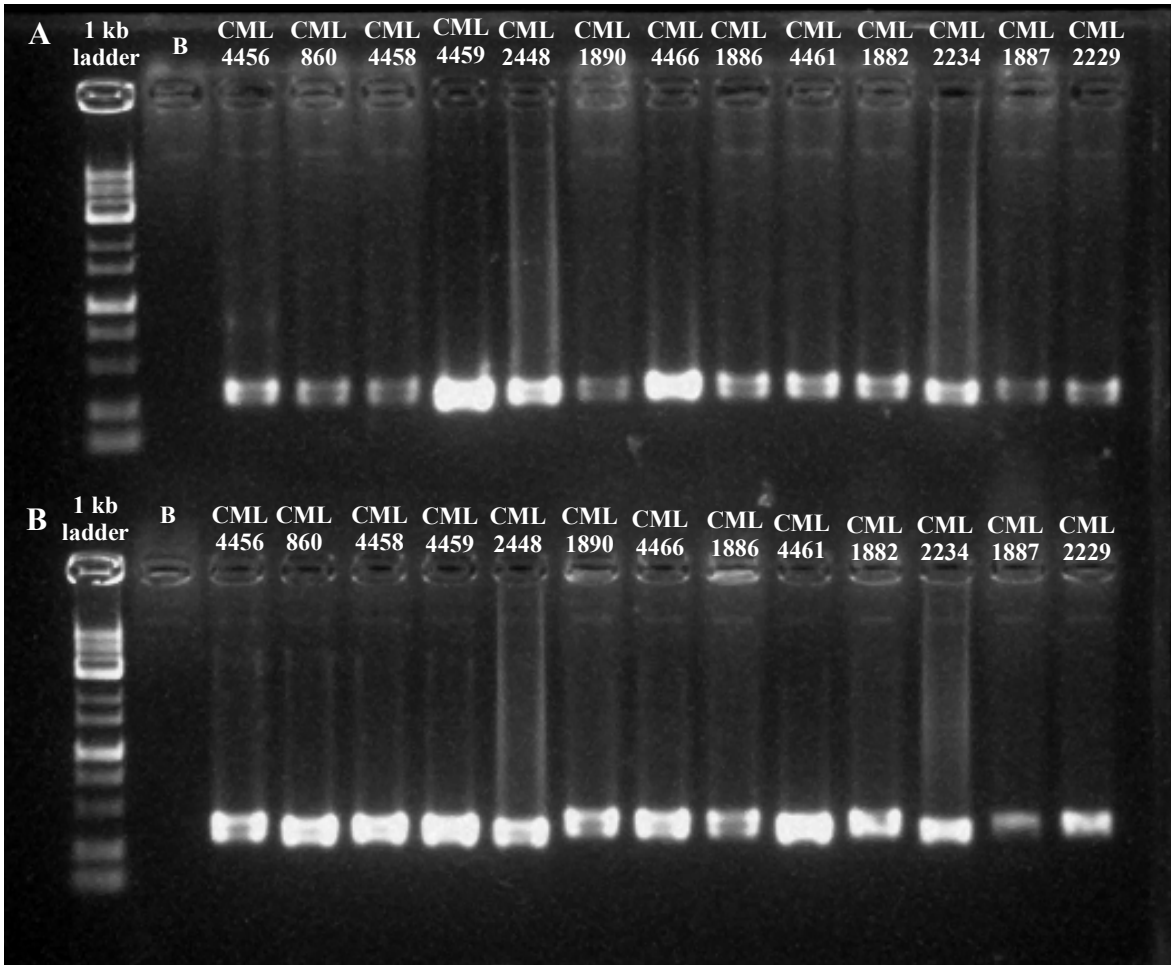

Figura 12. Resultado da amplificação de fragmento de dois genes que codificam toxinas em diferentes espécies de *Fusarium solani*. **A.** FvTox1. **B.** FvNIS1.

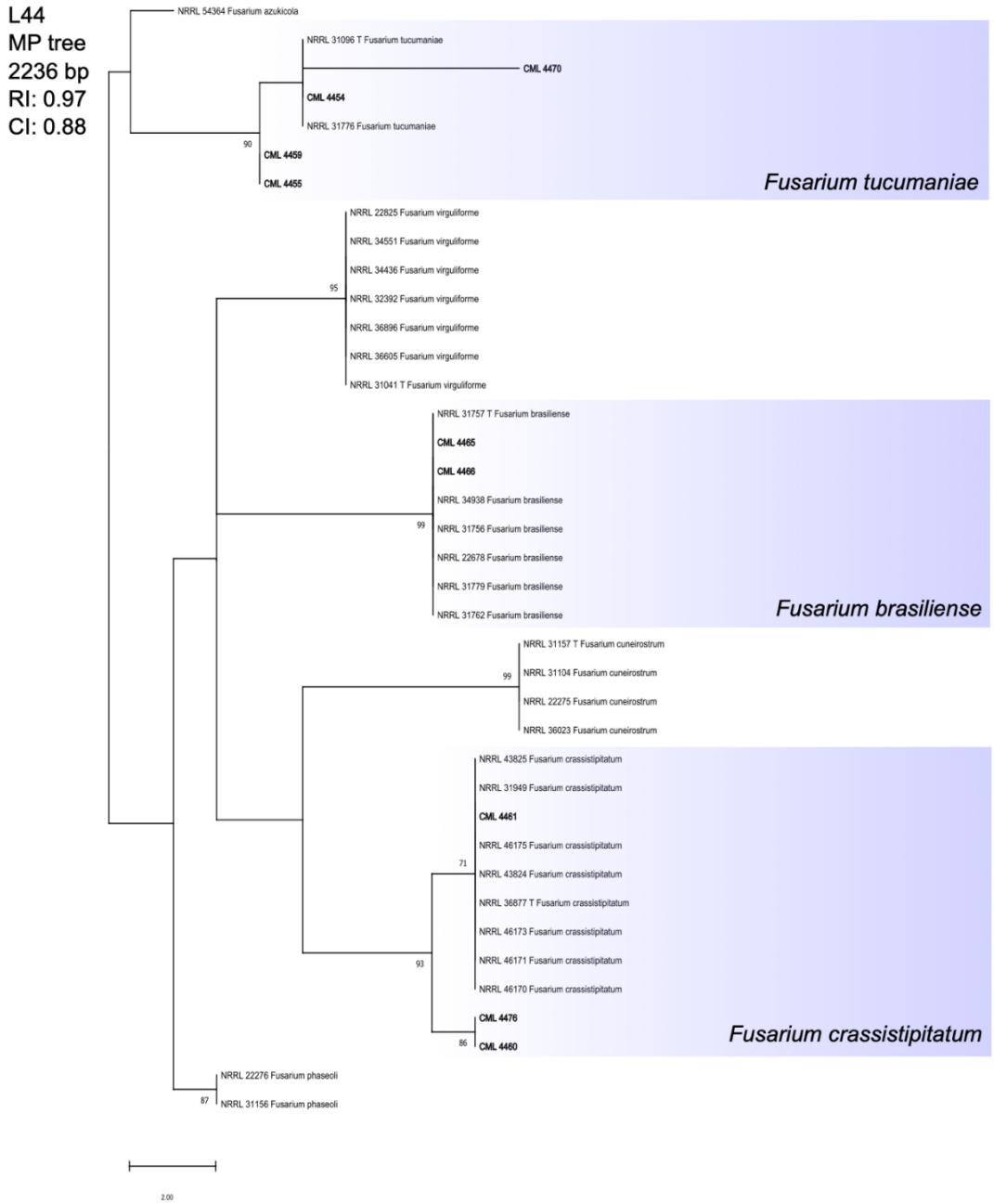

Figure S1. Maximum parsimony phylogenetic tree inferred from partial L44 sequences showing the relatedness of *Fusarium* species associated with soybean (*Glycine max* L.) with other clade 2 species from the *Fusarium solani* species complex. Bootstrap values ≥ 70% are shown at the internodes. Ex-type strains are indicated with T.

VITA

Ana Carolina Silva Galdino was born and raised in Ipatinga, Minas Gerais. In March 2011 she started her under graduation at Universidade Federal de Pelotas (UFPel). From 2014 to 2015 she studied Agriculture at Newcastle University, England, UK and got her degree in BSc. Agronomy by UFPel in March 2017. On August 2018 she started her post-graduation at Universidade Federal de Santa Catarina (UFSC) and on February 2020 she received a Master of Science Degree in Plant Genetic Resources. She started her PhD. in Plant Pathology at Universidade Federal de Lavras (UFLA) in March 2020. From 2022 to 2023 she was a Visiting Scholar at Purdue University, West Lafayette, USA. She presented her thesis on August 2024 at UFLA and became the first PhD. of her family.